Published in final edited form as:

Psychophysiology. 2014 November ; 51(11): 1072–1088. doi:10.1111/psyp.12288.

Taking the pulse of aging: Mapping pulse pressure and elasticity in cerebral arteries with optical methods

MONICA FABIANI[a,b,c,d], **KATHY A. LOW**[a], **CHIN-HONG TAN**[a,b], **BENJAMIN ZIMMERMAN**[a,d], **MARK A. FLETCHER**[a,d], **NILS SCHNEIDER-GARCES**[a,b], **EDWARD L. MACLIN**[a], **ANTONIO M. CHIARELLI**[a], **BRADLEY P. SUTTON**[a,c,d], **GABRIELE GRATTON**[a,b,c,d]

[a]Beckman Institute, University of Illinois at Urbana-Champaign, Urbana, Illinois, USA

[b]Psychology Department, University of Illinois at Urbana-Champaign, Urbana, Illinois, USA

[c]Bioengineering Department, University of Illinois at Urbana-Champaign, Urbana, Illinois, USA

[d]Neuroscience Program, University of Illinois at Urbana-Champaign, Urbana, Illinois, USA

Abstract

Cerebrovascular support is crucial for healthy cognitive and brain aging. Arterial stiffening is a cause of reduced brain blood flow, a predictor of cognitive decline, and a risk factor for cerebrovascular accidents and Alzheimer's disease. Arterial health is influenced by lifestyle factors, such as cardiorespiratory fitness (CRF). We investigated new noninvasive optical measures of cerebrovascular health, which provide estimates of arterial pulse parameters (pulse pressure, transit time, and compliance/elasticity) within specific cerebral arteries and cortical regions, and low-resolution maps of large superficial cerebral arteries. We studied naturally occurring variability in these parameters in adults (aged 55–87), and found that these indices of cerebrovascular health are negatively correlated with age and positively with CRF and gray and white matter volumes. Further, regional pulse transit time predicts specific neuropsychological performance.

Descriptors:

Aging; Cerebrovascular health; Arterial compliance; Cardiorespiratory fitness (CRF); Noninvasive optical imaging; Brain anatomy

Normal aging is often accompanied by changes in cognitive (Park et al., 2002; Salthouse, 2010; Schaie, 1989) and brain function (Alexander et al., 2012; Andrews-Hanna et al., 2007; Cabeza, 2002; Fabiani, 2012; Hedden & Gabrieli, 2004) as well as changes in the underlying brain tissue (Gordon et al., 2008; Pfefferbaum et al., 2000; Raz et al., 2010). These age-related effects are exacerbated in those older adults suffering from mild cognitive

Address correspondence to: Prof. Monica Fabiani, Beckman Institute, University of Illinois, 405 N. Mathews Ave., Urbana, IL, 61801, USA. mfabiani@illinois.edu.

Supporting Information

Additional supporting information may be found in the online version of this article:

Appendix S1: The use of photon (or phase) delay measurements to investigate the depth of the observed phenomena.

Figure S1: Optical pulsogram based on photon phase delay values.

impairment (MCI; Bennett et al., 2002; Gauthier et al., 2006; Hänninen, Hallikainen, Tuomainen, Vanhanen, & Soininen, 2002), a proportion of whom (> 50% within 5 years) converts to Alzheimer's disease (AD) or other forms of dementia (Grundman et al., 2004; Levey, Lah, Goldstein, Steenland, & Bliwise, 2006; Liddell et al., 2007; Lopez et al., 2003). Therefore, identifying predictors of age-related cognitive impairments can yield substantial societal and economic benefits by providing means of early detection and improving the chances of successful prevention and/or treatment.

Rapidly increasing evidence in humans and in animal models indicates that cardiorespiratory fitness level (CRF; Bherer, Erickson, & Liu-Ambrose, 2013; Hayes, Hayes, Cadden, & Verfaellie, 2013; McAuley, Kramer, & Colcombe, 2004; Voss, Vivar, Kramer, & van Praag, 2013) is one such predictor. Increased CRF can stave off or even reverse some of the negative effects of aging (Barnes, Yaffe, Satariano, & Tager, 2003; Colcombe et al., 2006; Erickson et al., 2009; Gordon et al., 2008; Voss, Heo et al., 2013). For example, extensive work has shown that highly fit older adults have more preserved white and gray matter in brain areas susceptible to age-related loss, such as frontal, parietal, and temporal cortex (including the hippocampus), as well as higher performance in neuropsychological and cognitive tasks, compared to age- and gender-matched low-fit older adults (Colcombe et al., 2006; Gordon et al., 2008). Highly fit older adults also display patterns of brain function more similar to those of younger adults (Hillman, Belopolsky, Snook, Kramer, & McAuley, 2004) and have more intact neurovascular coupling (Fabiani et al., 2014; see also Olopade et al., 2007; Safonova et al., 2004). Sedentary older adults who undergo a 6-month exercise intervention show reduced volumetric brain losses or even reversals in some cases (Colcombe et al., 2006; Erickson et al., 2011), and improvements in brain function and performance measures (Colcombe & Kramer, 2003; Hopkins, Davis, VanTieghem, Whalen, & Bucci, 2012; Tyndall et al., 2013; Voss et al., 2010). Finally, patients with higher CRF have higher cognitive performance than their low-CRF counter-parts, even when affected by AD (Heyn, Abreu, & Ottenbacher, 2004) or multiple sclerosis (Prakash, Snook, Motl, & Kramer, 2010).

Several, nonmutually exclusive factors have been implicated to explain the beneficial effects of CRF on cognition, brain anatomy, and brain function, including increases in trophic factors (such as the brain-derived neurotrophic factor, BDNF; Cotman, Berchtold, & Christie, 2007), spine, dendrite, and neuronal growth (Greenough & Volkmar, 1973; Jessberger & Gage, 2008), angiogenesis (Black, Isaacs, Anderson, Alcantara, & Greenough, 1990; Isaacs, Anderson, Alcantara, Black, & Greenough, 1992; Swain et al., 2003), and decreased arterial stiffness not only in older adults (Ferreira, Boreham, & Stehouwer, 2006) but also in young adults (Boreham et al., 2004). This latter factor, arterial stiffness, as well as other measures of cerebrovascular health, are of particular interest because a healthy cerebrovascular system is also critical for healthy cognitive and brain aging. Reduced cerebral blood flow (hypoperfusion; de la Torre, 1999) in aging is caused, among others, by hypertension (Jennings & Heim, 2012), arterio-sclerosis (i.e., arterial stiffness) and plaque formation (Boreham et al., 2004; Vaitkevicius et al., 1993). Arterial stiffness is predictive of cognitive decline (Unverzagt et al., 2011), is a critical risk factor for cerebrovascular accidents (Hatanaka et al., 2011; Mattace-Raso et al., 2006), and has been linked to the accumulation of beta-amyloid in AD (Casserly & Topol, 2004; Kalaria, Akinyemi, & Ihara,

2012). Maintaining a good level of CRF protects against the development or progression of arteriosclerosis (Ferreira et al., 2006).

This paper focuses on a new approach, based on optical imaging methods (E. Gratton et al., 1997), that allows us to investigate cerebrovascular health non-invasively (i.e., without the use of contrast agents or catheters). In particular, non-invasive (diffuse) optical methods (E. Gratton, Fantini, Franceschini, Gratton, & Fabiani, 1997)[1] can provide estimates of arterial elasticity and cerebral pulse pressure in different cortical regions, pulse transit time from the carotids to the head and within large cerebral arteries, and also allow us to visualize large superficial arteries running along the cortical surface.

In clinical practice, arterial elasticity is typically estimated noninvasively on the basis of particular patterns of variations of blood pressure during a pulse cycle. Specifically, elasticity is inferred by a prolongation or secondary peak during the systolic relaxation phase of the pulse (backward or reflected wave; see Izzo & Shikoff, 2001). Systemic estimates of arterial elasticity may be obtained inexpensively using measures of pulse pressure (i.e., the difference between systolic and diastolic blood pressure, which increases with aging; e.g., Izzo & Shikoff, 2001). Arterial elasticity can also be measured at the carotids using Doppler ultrasound technology (Calabia et al., 2011; Keller, Meier, Anliker, & Kumpe, 1976). Other estimates of arterial elasticity can be obtained by measuring pulse wave velocity in the aorta (aPWV; Asmar et al., 1995; Blacher, Asmar, Djane, London, & Safar, 1999) and at the femoral artery, and by calculating the difference in timing and distance between the two. Faster PWVs correspond to stiffer arteries and are associated with an increased risk of mortality (Blacher, Guerin et al., 1999; Willum-Hansen et al., 2006).

Noninvasive measures of cerebral arterial elasticity are more limited. Transcranial Doppler can be used to derive intracranial measures of elasticity (Keage et al., 2012) and cerebral blood pressure (Asgari et al., 2012). However, this method has a limited viewing window that restricts the measurement to a few major deep arteries within the skull, and it is not suitable for relatively small vessels, whose flow direction is variable and whose flow velocity is relatively low. Other noninvasive imaging techniques, such as magnetic resonance imaging (MRI), are very useful for studying other parameters of cerebral blood circulation and blood flow, using arterial spin labeling (ASL; Calamante, Thomas, Pell, Wiersma, & Turner, 1999; Z. Wang et al., 2013) or similar sequences. The optical methods presented in this paper may enable complementary assessments of the state of the cerebrovascular system and could in principle be recorded concurrently with both Doppler and MR data.

Optical methods have been used to study pulse parameters and blood oxygenation in the periphery for decades (e.g., photoplethysmography; Alian & Shelley, 2014; Allen, 2007) and have been shown to yield waveforms very similar to those obtained with continuous-wave Doppler (Cook, 2001; Wisely & Cook, 2001; a typical Doppler wave is displayed in Figure 1A). These methods are based on measuring changes in near-infrared (NIR) light absorption that occur as a function of changes in the concentration of oxy- and deoxyhemoglobin

[1]The term *diffuse* refers to a type of noninvasive optical imaging conducted in highly scattering media, such as the human body. Functional near-infrared spectroscopy (fNIRS) is a diffuse optical imaging method, as are the fast optical signal (FOS) and the event-related optical signal (EROS). Here, we use the term *optical imaging* to indicate these types of measures.

(functional near-infrared spectroscopy, fNIRS; Hoshi & Tamura, 1993; Murkin & Arango, 2009; Villringer & Chance, 1997). The pulsation of blood in arteries and arterioles induces changes in the amount of light absorption, which can be measured at high sampling rates (up to thousands of times per second). Therefore, the pulse cycle recorded optically can be studied in exquisite detail even in single trials (Gratton & Corballis, 1995; see Figure 1B). It is important to note that pulse parameters can be recorded concurrently with fNIRS measurements using the same instrumentation. When the focus is on hemodynamic measures of brain function, the pulse is treated as a nuisance variable and eliminated from the data (Gratton & Corballis, 1995; Huppert, Diamond, Franceschini, & Boas, 2009). However, it can also be analyzed as the target signal when, as in this case, the focus is on cerebrovascular health.

A few recent papers have also examined the optical pulse within the brain. For example, Themelis et al. (2007) showed the feasibility of using an optical approach in neonatal pigs. The results indicated that, given appropriate source-detector distances, the signal contribution of the scalp was minimal, reflecting instead the effects of cerebral hemodynamics. They also confirmed the fact that Doppler and optical data were highly correlated. Ebihara and colleagues (2013) analyzed the power spectrum of the pulse wave from frontotemporal regions in patients suffering from cerebral ischemia and reported that the transmission of the pulse wave was attenuated in the region with reduced blood flow.

The measurement approach proposed here represents an extension of the optical work described above and applies it to the mapping and measurement of a number of cerebral pulse parameters, including pulse pressure, arterial elasticity, and pulse transit time (the inverse of PWV), measured at the carotids and regionally within the human cortex. This is made possible by the use of an extensive (high-density) array of optical sensors (sources and detectors located on the scalp at a few centimeters distance from each other; see Figure 1E) covering the entire head surface (see Baniqued, Low, Fabiani, & Gratton, 2013; Tse, Low, Fabiani, & Gratton, 2012). This enables the measurement of the pulse cycle from many different locations across the head surface and, through the identification of specific arteries, allows for the separation of signals into intra- and extracranial sources.

The pulse parameters we are using in this study are all indices of cerebrovascular health and arterial elasticity. Pulse transit time is inversely proportional to PWV: the longer the pulse transit time, the more elastic are the large arteries in the head. The amount of drop in light intensity that occurs during systole, referred to here as *pulse amplitude*, is a measure of the momentary distension of the arteries resulting from the passing of the pulse pressure wave, which absorbs more of the light traveling between the source and the detector (Figure 1B, systole). Pulse amplitude over the head averages approximately 0.6% of the average light intensity. This value, however, is larger over large arteries than when measured over arterioles. This makes it possible to visualize large arteries, such as the outer branches of the middle cerebral artery (MCA), using maps of pulse amplitudes (referred to here as *pulsograms*) that are appropriately thresholded to show locations at which the pulse amplitude is largest. After reaching its systolic peak minimum, light intensity begins to grow again as the blood pressure wave dissipates (Figure 1B, diastole). This occurs in different ways depending on how elastic or sclerotic the arteries are. In general, the effect of arterial

elasticity is to diffuse the pulse over time, generating a smaller systolic deviation and a slower return during the diastole. This is typically referred to as *arterial compliance* (Liang, Teede, Kotsopoulos, & Shiel, 1998).

In order to assess the validity of this approach, we measured these parameters in a sample of healthy middle-aged and older adults varying in CRF. In the same participants, we also obtained measures of performance in a neuropsychological test battery, estimates of brain volumes obtained with FreeSurfer (Dale, Fischl, & Sereno, 1999; Fischl et al., 2002), and blood flow estimates obtained with ASL.

Method

Participants

Fifty-three adults (aged 55–87, 27 females, evenly distributed over the age range and by gender) were admitted into the study after meeting all inclusion and exclusion criteria. This age range was chosen because it encompasses the typical time period in which the effects of changes in arterial elasticity become more obvious, with enough individual differences to examine variability. All participants were right-handed (as assessed by the Edinburgh Handedness Inventory; Oldfield, 1971), had normal or corrected-to-normal vision, and were native speakers of English. Exclusionary criteria included serious medical conditions, a history of major neurological or psychiatric disease, or a history of drug abuse. Additionally, participants were screened and excluded from participation if they showed signs of dementia (a score below 51 on the modified Mini-Mental Status examination—mMMS; Mayeux, Stern, Rosen, & Leventhal, 1981) or depression (a score above 14 on Beck's Depression Inventory; Beck, Steer, & Brown, 1996). Participants who smoked more than half a pack of cigarettes and/or consumed more than two alcoholic drinks per day were also excluded. Additionally, participants were excluded if they used medications affecting the central nervous system. All prescription medications were recorded. Thirty-two percent of the participants reported taking blood pressure medications. Participants' blood pressure was taken at three time points across the experiment and averaged to provide measures of systolic and diastolic blood pressure. Peripheral pulse pressure was derived by taking the difference between systolic and diastolic blood pressure.[2] Body mass index (BMI) was also calculated for each participant. All participants were recruited from the Champaign-Urbana community, were paid for their participation, and signed informed consent in accordance with the University of Illinois at Urbana-Champaign's Institutional Review Board. Demographics and neuropsychological data for this sample are reported in Table 1.

Assessment of cognitive function.—Participants were administered a battery of neuropsychological tests, which included the Kaufmann Brief Intelligence Test (K-BIT; Kaufman & Kaufman, 2004), the Shipley's vocabulary test (Shipley, 1940), to measure IQ and vocabulary, respectively; the Wisconsin Card Sorting Test (WCST, Heaton, 1981; Tien et al., 1996), the Verbal Fluency Test (letters CFL; Benton & Hamsher, 1989), the

[2]The use of blood pressure medications was not correlated with pulse pressure (measured at the forearm) nor with optical cerebral pulse amplitude measures, but was marginally negatively correlated with indices of arterial elasticity ($r = -.25$ for compliance and $r = -.26$ for pulse transit time, both $p < .10$).

operation-span task (OSPAN; Unsworth, Heitz, Schrock, & Engle, 2005) and the Trail Making Tests A and B (Corrigan & Hinkeldey, 1987), to measure working memory and executive function. In addition, scores for forward and backward digit span were derived from the mMMS.

Assessment of cardiorespiratory fitness.—The gold standard measure for CRF is VO_{2max}, a measure of the maximum oxygen consumption in an individual's body obtained during a maximal graded bout of exercise. However, older and low-fit individuals may have conditions that prevent them from participating in such a stressful exercise routine. Since these individuals are of crucial interest for the examination of the relationship between cardiores-piratory fitness, aging, and cerebrovascular health, we estimated CRF according to an equation that utilizes easily acquired parameters that are highly predictive of VO_{2max} (Jurca et al., 2005; Stamatakis, Hamer, O'Donovan, Batty, & Kivimaki., 2013). This measure is obtained from a linear combination of weighted variables, including gender, age, BMI, resting heart rate, and a physical activity score, plus a numerical constant. This CRF index, expressed in metabolic equivalents, has been demonstrated to approximate VO_{2max} with good accuracy in a large sample ($N > 40{,}000$), with correlations approximately of .7 or higher. Recently, Mailey et al. (2010) extended the validity of the CRF estimate specifically to 172 older adults, ranging in ages from 60–80 (see also McAuley et al., 2011). Since CRF (like VO_{2max}) is systematically larger in men than in women (Jurca et al., 2005) we partialled out gender in some of the analyses to avoid potential biases.

Experimental Procedures and Types of Measures

The data presented here were collected as a part of a much larger, multisession experiment intended to investigate cerebrovascular reactivity. Session 1 included neuropsychological assessments and familiarization to MRI scanning within a mock magnet. Session 2 included the collection of structural MRI data (used for anatomical coregistration and brain volume estimation) and hemodynamic flow data using arterial spin labeling (ASL). The optical imaging data were collected in Session 3 and included optical measurements taken at the scalp and over the left carotid artery as well as an electrophysiological measurement of the heartbeat.

Electrocardiogram Recording and Analysis

Lead I of the electrocardiogram (EKG, left wrist referenced to right wrist) was recorded using a Grass Model 12 amplifier with a sampling rate of 200 Hz and a band-pass filter of 0.1 Hz to 100 Hz. The EKG lead was recorded in order to synchronize the optical pulse data to the R wave (to ensure that the same pulse was examined regardless of location). The exact timing of each R-wave peak was found by searching for peak points exceeding a certain voltage threshold (scaled for each subject) and dismissing any points outside the normal range of interbeat intervals. Proper identification was subsequently ensured by manual inspection, and any false detections (e.g., a large T wave inadvertently identified as an R wave) were eliminated.

Optical Recording and Analysis

Recording.—Optical data were recorded with six integrated frequency domain oxymeters (Imagent; ISS, Inc., Champaign, IL). Data were collected from 24 detectors each measuring light emitted by 16 time-multiplexed sources (384 channels). Laser diodes generated light at 830 and 690 nm (max amplitude: 10 mW, mean amplitude after multiplexing: 1 mW), modulated at 110 MHz. The light from the diodes was transmitted to the surface of the head using optical fibers (one per emitter, with separate fibers carrying light at each of the two wavelengths coupled at each location). Each optical fiber carrying the light to the surface of the head was 400 μm in diameter. Light was collected from the head using detector fiber bundles measuring 3 mm in diameter and connected to photomultiplier tubes (PMTs). Sources and detectors were held flush with the participants' scalp using a modified motorcycle helmet. A fast Fourier transform of the output data from the PMTs was used to calculate DC (average) intensity, AC (amplitude), and relative phase, or photon, delay (in picoseconds; see online supporting information for additional details). The majority of the analyses reported here are based on the AC intensity values. Optical parameters were sampled at 39.0625 Hz (25.6 ms per sampling point). The arterial pulse is the largest phenomenon that can be measured using AC intensity, being easily visible on single trials.

The pulse wave was also recorded at the left carotid with an Oxiplex TS (ISS, Inc., Champaign, IL) using one detector and a pair of sources (830 and 690 nm) mounted in a small rubber patch and taped to the neck, with a source detector distance of 1.3 cm. The exact location was adjusted until a clear pulse was visible. The carotid data were collected with a sampling rate of 50 Hz (20 ms sampling period).

Coregistration with structural MRI.—Using nasion and preauricular points as references, the locations of individual optical sources and detectors were digitized using a Polhemus "3Space" FASTRAK 3D digitizer (Polhemus, Colchester, VT). T1-weighted structural magnetic resonance images were obtained for each subject. The MPRAGE images were aligned on the anterior and posterior commissures using AFNI (Analysis of Functional NeuroImages; Cox, 1996). The Polhemus digitization points were then coregistered with the transformed MR images first using the three fiducial markers and then surface fitting the entire set of digitized points to the estimated scalp surface based on a Levenberg-Marquardt algorithm (least-squares fit), which has been shown to have errors of less than 4 mm (Whalen, Maclin, Fabiani, & Gratton, 2008). Figure 1E depicts the recording montage (and additional digitized points) superimposed on the structural MRI of one representative participant.

Measurement of pulse parameters.—Measurements were taken at rest during six periods of 12 s each for a total of 72 s of recording. The optical data were normalized (by dividing them by their mean value) and band-pass filtered between 0.5–5 Hz. This allowed us to compare channels with different amounts of light within and across participants. The pulse waveform was obtained from each optical channel by averaging the AC light intensity time locked to the peak of the R wave of the EKG (signalling the depolarization of the ventricular myocardium, and ensuring that we were measuring the same pulse cycle at different locations). Pulse waveforms from each channel were then projected onto an

ellipsoid of the head surface, which was determined by the locations of the corresponding sources and detectors. For the majority of points, the ellipsoids corresponding to multiple channels overlapped. In those cases, the data from the overlapping channels were integrated (using the product of different channel values for AC intensity data, see Wolf et al., 2000). For regional measures, the pulse waveforms for points corresponding to various cortical regions as identified through the Talairach atlas (Talairach & Tournoux, 1988) were averaged together. The corresponding waveforms observed at different locations were used for pulse quantification. Only source-detector distances between 2 and 6 cm were used in the analysis, allowing us to image phenomena occurring approximately between 1 and 3 cm in depth.

Prior to analysis, the pulse waveforms were baselined by dividing them by the average value during an interval between 100 and 200 ms after the EKG R-wave peak (corresponding, in most cases, to the diastolic maximum of the previous pulse cycle). Thus, the waveforms are expressed as proportional (or percent) changes with respect to this period. We then derived optical pulse parameters as follows: (a) for pulse amplitude, we considered the percent difference between the minimum (systole) and the baseline value of the optical pulse waveform; (b) for transit time, we used the onset latency of the systole (identified as the point of maximum diastolic value in the preceding pulse wave, corresponding to the onset of the new systolic pulse) and compared this latency to either the EKG R wave or to the onset latency of the systole at other locations; (c) to provide an initial estimate of arterial compliance and elasticity, we used a simplified Windkessel approach based on the difference between two areas: (1) an area corresponding to the integrated AC intensity values between the systolic peak and the next diastolic peak; and (2) the area of a triangle identified by the systolic and diastolic peaks and a point corresponding to the diastolic value reported at the time of systolic peak (see Figure 2A). The difference between these two areas (the green area in Figure 2A) was then normalized, by dividing it by an estimate of pulse peak amplitude (based on the difference between the systolic peak and subsequent diastolic peak).[3]

To obtain the optical arterial map, or pulsogram, we used the following procedure. First, for each voxel, we computed the normalized amplitude of the pulse (i.e., the mean AC amplitude between 384 and 538 ms after the R wave of the EKG), averaged across participants. Second, we spatially high-pass filtered the maps so as to enhance the contrast between voxels with high pulse values and voxels with low pulse values. This was done by subtracting, from the AC value observed at each pixel, the average AC value of all pixels surrounding it, with a distance less than 2.25 cm. Third, we thresholded the image, so that only pixels with values greater than a criterion (~ 0.5% of the diastolic intensity value) are plotted.

[3]The Windkessel model assumes that the relaxation of the blood vessels during the diastole should follow an exponential function, whose parameters are related to the compliance of the vessels. Here, however, we are not attempting to distinguish between compliance and elasticity. Therefore, to simplify computation, we used a straight line to estimate the relaxation function, which in turn is subtracted from the actual data to estimate the reflected wave.

MRI Recording and Analysis

MRI recording.—A high-resolution structural MR scan was collected on a 3T Siemens Trio scanner using a standard body coil transmission and a 12-channel head array receiver coil. The T1-weighted brain image was acquired using a 3D MPRAGE (magnetization prepared rapid gradient echo) protocol (TR = 1,900 ms, TI (inversion time) = 900 ms, TE = 2.32 ms, field of view (FOV) = 230 × 230 × 172.8 mm^3 (sagittal), matrix size = 256 × 256 × 192, flip angle = 9°, slice thickness = 0.9 mm).

In addition to the anatomical scans, we also recorded blood flow data. Six axial imaging slices passing through the middle of the lateral ventricles and covering part of the frontal cortical areas were acquired with a localized pseudocontinuous transfer insensitive labeling technique (pTILT; Ouyang & Sutton, 2011) ASL sequence, and the labeling slice was placed inferior to the imaging slab with a 10-mm gap. To minimize motion, padding was used to stabilize the subject's head. The imaging and tagging parameters of the localized pTILT ASL sequence were: windowed-sinc 45° RF pulses with 2,560-μs duration, tagging repetition spacing = 30 ms, number of concatenated RF pulse pairs = 100, tagging duration = 3 s, postlabeling delay = 0.5 s, tagging slice thickness = 10 mm, gradient spoiler duration and amplitude = 4,000 μs/[± 10, ± 12, ± 14, ± 16] mT/m, SE-EPI readout, FOV = 220 × 220 mm, scan matrix size = 64 × 64, TR/TE = 4,500/44 ms, slice thickness = 6 mm, slice gap = 1.2 mm, 36 control and 36 tag repetitions, scan time of one acquisition = 5 min, 24 s.

Finally, in order to provide a comparison with the arterial maps derived from the optical data, we collected one MR-based arteriogram from a single participant with a time-of-flight 3D angiography sequence, using a parallel imaging factor of 2, and obtaining a 0.9-mm isotropic resolution. This sequence shows large and small arteries and can be easily registered to the MPRAGE for anatomical localization. Since the optical measurements can only visualize relative superficial arteries, we developed a procedure to avoid the contribution of deep arteries (i.e., arteries located more than 5 cm below the scalp surface). The arteriogram was coregistered to the T1 anatomical image of the same participant. It was then high-pass filtered by subtracting a smoothed image (9 mm 3D moving average low-pass filter) from the original image. The arteriogram was then masked using a scalp extraction and brain segmentation procedure. The MRI scalp was derived using the algorithm described by Whalen et al. (2008). We then shrank the extracted scalp in order to define an "inner region" with a fixed distance from the original scalp to mask deep arteries. The resulting image was then thresholded by visual inspection in order to obtain optimal visualization of the superficial cerebral arteries.

ASL data processing.—pTILT data processing was carried out using SPM-8 (Wellcome Department of Cognitive Neurobiology, University College of London, UK) and FSL 4.1.4 (FMRIB Software Library; http://www.fmrib.ox.ac.uk/fsl). fMRI modeling of the perfusion level was determined using the general linear model with the ASL modeling framework described by Hernandez-Garcia, Jahanian, and Rowe (2010). The unsubtracted pTILT data were first realigned to remove motion artifacts. After regression analysis, gray and white matter masks were formed from segmenting the T1 structural scan using FSL's FAST software (Zhang, Brady, & Smith, 2001). The gray and white matter masks were then

transformed into the subject's pTILT space using a registration between the control image in pTILT and the MPRAGE from FSL's FLIRT (Jenkinson & Smith, 2001).

Volumetric analyses.—Cortical reconstruction and volumetric segmentation were performed with the FreeSurfer (5.0) image analysis suite (http://surfer.nmr.mgh.harvard.edu/; e.g., Dale et al., 1999; Fischl & Dale, 2000; Fischl, Liu, & Dale, 2001; Fischl et al., 2002; Han et al., 2006). This method uses both intensity and continuity information from the entire three-dimensional MR volume in segmentation and deformation procedures to produce representations of cortical thickness, calculated as the closest distance from the gray/white boundary to the gray/cerebral spinal fluid boundary at each vertex on the tessellated surface (Fischl & Dale, 2000). Procedures for the measurement of cortical thickness have been validated against histological analysis (Rosas et al., 2002) and manual measurements (Kuperberg et al., 2003). FreeSurfer morphometric procedures have been demonstrated to show good test-retest reliability across scanner manufacturers and across field strengths (Han et al., 2006). The automatic segmentation performed by FreeSurfer was extensively examined for errors. Any errors found were corrected according to the instructions found at http://surfer.nmr.mgh.harvard.edu/fswiki/FsTutorial/TroubleshootingData. All data presented in this paper were normalized by head size.

Statistical Analyses

Most of the analyses reported here were based on the computation of the Pearson's product-moment correlation coefficient (r), followed by two-tailed t-test analyses to evaluate whether the values differed from 0. All of the analyses presented here tested a priori hypotheses of the relationships between variables based on the extant literature. As such, they should be considered as separate tests and not corrected for multiple comparisons.

Results

The main correlations among variables that are detailed in the following Results section are also reported in summary form in Table 2.

Basic Effects of Age and CRF

In this section, we briefly review data indicating that our sample exhibits the typical effects of aging and CRF commonly described in the literature. As expected, age and CRF showed correlations between each other and with many other variables. Age was negatively correlated with CRF, both in terms of the raw score, $r(51) = -.415$, $p < .005$, and when fitness was adjusted by gender, $r(51) = -.460$, $p < .001$. Age had a strong effect on brain volumetric measures, $r(51) = -.499$, $p < .0001$, for cortical gray matter volume; $r(51) = -.560$, $p < .001$ for white matter volume; and $r(51) = -.313$, $p < .05$ for subcortical gray matter volume. These correlations extended to the majority of the specific cortical regions measured. However, since these relationships are well documented in the literature and they are the focus of another paper (Fletcher et al., in preparation), we will not report them here in further detail. Cardiorespiratory fitness effects on volumetric brain measures were more circumscribed. Specifically, fitness effects were stronger than age effects in subcortical gray

matter, $r(51) = .419$, $p < .002$, suggesting a focused effect of CRF on this brain region, which went beyond the general relationship between age, fitness, and brain anatomy. This is consistent with previous reports (e.g., Erickson et al., 2009).

Also as expected, both age and CRF were correlated with performance in the neuropsychological test battery (see Table 3). Again, as these phenomena are not the target of the present paper, we will not comment on them further.

Carotid Pulse Parameters

The grand-average pulse waveforms from the carotid and from the scalp (averaged across scalp locations) are presented in Figure 2B. Only participants for whom both carotid and scalp measures were available were used for this figure ($N = 37$).[4] These waveforms show the typical optical pulse shape, and suggest that the amplitude of the pulse (expressed as a percentage of the maximum diastolic value) was similar at the carotid and at the scalp. However, there were subtle differences in the timing and shape of the two waveforms. The onset of the descending (systolic) part of the pulse waveforms occurred earlier (by 99.97 ± 49.38 ms) for the carotid pulse than for the pulse measured over the scalp, $t(29) = 11.09$, $p < .0001$. This interval can be considered as an estimate of the pulse transit time, that is, the time taken by the pulse wave to travel from the neck to the head. As pulse transit time is easier to measure in our data than pulse wave velocity (as the exact length of the arteries between the neck and the head is difficult to assess), we will use this variable rather than PWV in further analyses.

Figure 3A shows a scatter plot depicting the relationship between carotid pulse amplitude and pulse pressure (i.e., the difference between systolic and diastolic blood pressure). These data indicate that the carotid pulse amplitude was well correlated with peripheral pulse pressure: $r(35) = .625$, $p < .0001$. In fact, this correlation is comparable with the test-retest reliability of pulse pressure measured with a sphygmomanometer at the arm in our study ($r = .67$). Figure 3B shows a scatter plot of the relationship between carotid pulse amplitude and age (the relationship between pulse pressure and age is shown in Figure 3C). As expected, these figures show that age is correlated with pulse pressure, $r(51) = .306$, $p < .05$, and with carotid pulse amplitude, $r(35) = .455$, $p < .005$. These data provide support to the claim that carotid pulse amplitude measured with diffusive optical methods is related to pulse pressure.

Interestingly, carotid pulse amplitude was not significantly correlated with CRF for the raw scores, $r(35) = .160$, or for the scores adjusted by gender, $r(35) = .112$. There were also no significant correlations between carotid pulse amplitude and volumetric brain measures. Finally, none of the correlations with neuropsychological variables reached significance.

In addition to pulse amplitude, we also measured arterial compliance/elasticity. Figure 2C shows examples of cerebral pulse waveforms in two participants with high and low compliance values (for illustration purposes, these participants were chosen because they have a similar heart rate). The compliance value at the carotids was marginally correlated

[4]Carotid data were only available from 37 participants. The rest of the participants were discarded due to excessive movement artifacts and/or poor contact between the probe and the neck. Onset data could not be computed reliably from 7 additional participants, reducing the N to 30 for those analyses.

across participants with their carotid pulse amplitude, $r(35) = -.319$, $p = .054$. It was, however, strongly correlated with the onset latency of the pulse wave (i.e., with the interval between the EKG R wave and the onset of the pulse pressure wave in the carotid; $r(28) = .513$, $p < .001$). This latter measure may be considered as dependent on the velocity of the pulse wave in its initial tract over the ascending aorta and the common carotid artery, which, similar to compliance measures, should depend on the elasticity (or lack thereof) of the arteries. Compliance estimates at the carotid did not significantly correlate with age, $r(35) = -.13$, *n.s.*, or CRF, $r(35) = .04$, *n.s.*, and were not a significant predictor of volumetric brain measures (all $rs < .30$). There was, however, a significant correlation between carotid compliance estimates and performance in the forward digit span test, $r(37) = .368$, $p < .05$.

Cerebral Pulse Parameters

The pulse can be easily measured, even without averaging, from sources and detectors located on the surface of the head (see Gratton & Corballis, 1995). For the purposes of the current paper, however, it is critical to show that the pulse measured in this fashion is generated inside the skull, and therefore reflects arteries that bring blood directly to brain tissue. Previous studies (Ebihara et al., 2013; Themelis et al., 2007) have already shown that this is a reasonable assumption. Here, we use three different types of data to support this argument:

1. Figure 4B shows an optically derived pulsogram (i.e., a map of the superficial arteries derived from the optical pulse amplitude), averaged across the participants in the study. Figure 4A shows the MRI-based arteriogram of one participant in which only arteries running superficially over the brain are shown. A clear similarity can be seen between the two maps, although the optical map is smeared due to the fact that it was averaged across participants and that the spatial sampling of the optical data was much lower than that of the MR data. Two arteries are highlighted in the MR arteriogram (Figure 4A): the left middle cerebral artery (MCA) and the precentral artery (PCA). These arteries have been selected because they feed areas of the cortex that are important for language production (MCA) and for attention/working memory (PCA). Both arteries are clearly visible in the pulsogram. The MR arteriogram also reveals other arteries, including the anterior cerebral artery and the central artery. All these arteries are also visible, at least in part, in the pulsogram. The pulsogram also reveals a posterior vertical band, which is not clearly visible in the arteriogram. This may be composed of the ascending portion of the posterior parietal artery and the descending portion of the posterior temporal artery, which may be difficult to visualize using the MR arteriogram due to the slow blood flow velocity in these vessels (as these are secondary branches of other larger arteries).

2. The flow of the pulse wave along the arteries is generally consistent with the known direction of flow for arteries inside the skull and not with that of arteries outside the skull. The direction of flow is illustrated in Figure 4C, showing a time-resolved pulsogram. This map was obtained by plotting, for each voxel, thresholded according to the procedures described above, the latency (from the EKG R wave) of the peak of the pulse instead of its amplitude. For instance,

for the superficial branch of the MCA (highlighted in Figure 4), the flow of the pulse proceeds from its point of emergence on the surface of the head (inferior frontal/anterior temporal lobe) in a posterior direction running over the temporal lobe. Interestingly, the flow on the large posterior band appears to proceed from a point in the middle (in green in Figure 4C) toward both the top and the bottom (in red in Figure 4C). This is consistent with the interpretation that this band is made up of two diverging branches, one moving up (the posterior parietal artery) and the other moving down (the posterior temporal artery).

3. The pulse obtained by imaging the phase/photon delay (instead of the AC) parameter is always showing a reduction in phase during the systole across the whole head, supporting the idea that these arterial pulse effects are generated inside the skull (see supporting information for additional details).

Another method for distinguishing deep and superficial effects is to map separately very short (source-detector distance less than 2 cm) and long (source-detector distance more than 2 cm) channels (see Themelis et al., 2007). However, in this study we did not have a sufficient number of short channels to obtain reliable maps of the superficial (extracranial) arteries, as we only considered source-detector distances exceeding 2 cm.

Taken together, these data provide strong support to the claim (already present in the literature; Ebihara et al., 2013; Themelis et al., 2007) that the cerebral optical pulse is generated, at least in part, by arteries running along the external surface of the brain inside the skull. They also show that it is possible to generate maps of arterial pulse parameters using optical measures (pulsograms). These maps can visualize both the amplitude of the pulse (which is related to pulse pressure within the various arteries that are measured) and its timing (in the case shown, the latency of the pulse peak).

Figure 2D shows the pulse waveform computed separately for oxy- and deoxyhemoglobin measures. As is evident from this figure, the pulse is almost entirely related to changes in oxyhemoglobin concentration, with minimal effects carried by changes in deoxyhemoglobin. In other words, it is a phenomenon related to blood highly saturated in oxygen (on average 97.9%, $SD = 4.1\%$)—such as the blood that is carried through by arteries. This is consistent with the idea that the measurements refer to arterial rather than capillary pulsations.

Relationship between average cerebral pulse amplitude and other variables.— The amplitude of the average cerebral pulse (i.e., the difference between the diastolic and systolic peak values averaged across all brain areas) was correlated with the amplitude of the pulse at the carotid, $r(35) = .512$, $p < .001$. It was also correlated with pulse pressure measured with the sphygmomanometer at the arm, $r(51) = .380$, $p < .001$. Both of these relationships support the idea that optical cerebral pulse amplitude is a proxy measure of pulse pressure within the arteries flowing around the brain. Consistent with this claim, the cerebral pulse amplitude was also correlated with age, $r(51) = .302$, $p < .05$, with pulse amplitude increasing with increasing age. However, the cerebral pulse amplitude was not significantly correlated with blood flow measures computed with ASL-MRI, $r(38) = -.042$

for gray matter, and $r(38) = -.181$ for white matter, both *n.s.*, CRF ($r = .083$, *n.s.*), global anatomical measures ($|r| < .134$, *n.s*), or neuropsychological variables ($|r| < .180$, *n.s.*).

Optical measures of cerebral arterial elasticity.—We selected two measures of cerebral arterial elasticity: Measures of arterial compliance computed globally over the whole head and measures of pulse transit time computed both globally and at specific locations within the head. Examples of arterial compliance maps (not thresholded by amplitude, and thus combining large and small arteries) from four individual participants varying in age and CRF level are shown in Figure 5. In the remainder of this section, we will present data about the relationship between parameters of the cerebral arterial pulse and other vascular parameters, age and CRF, brain anatomy, and function.

As predicted, arterial compliance measured globally over the head was inversely correlated with age, $r(51) = -.390$, $p < .005$, and positively correlated with CRF, $r(51) = .416$, $p < .005$. It was also significantly correlated with pulse transit time at the carotid, $r(35) = .348$, $p < .05$, but not with compliance estimated at the carotid, $r(35) = .190$, *n.s.* The global compliance estimate was not significantly correlated with blood flow (measured by ASL MRI), $r(38) = .198$, *n.s*). The global compliance estimate was a significant predictor of global brain volumetric measures, $r(51) = .299$ for cortical gray matter; $r(51) = .443$ for white matter volume; and $r(51) = .354$ for subcortical gray matter, all ps $< .05$ (see Figure 6). The global compliance estimate also showed significant correlations with volumetric measures from several specific brain regions, the most notable being hippocampal volume, $r(51) = .457$, $p < .0005$, and entorhinal cortex volume, $r(51) = .445$, $p < .0005$. Finally, compliance was negatively correlated with several error-related scales of the WCST, reflecting lack of cognitive flexibility for subjects with low arterial compliance/elasticity. These included number of trials, number of errors, number of perseverative responses, number of perseverative errors, and percent perseverative errors, all $r(51) < -.282$ ($p < .05$).

Global cerebral pulse transit time was calculated by subtracting the onset time of the systolic pulse in the carotid measures from the onset time of the average systolic pulse in the cerebral measures. Therefore, pulse transit time was only available for those participants in which the onset latency of the carotid pulse measure could be estimated ($N = 30$). When averaged across the whole head, this measure was significantly correlated with CRF, $r(28) = .387$, $p < .05$, but not with age, $r(28) = -.126$, *n.s.*, with ASL mean blood flow measures in the gray, $r(28) = .345$, $p < .05$, one-tailed, and white matter, $r(28) = .467$, $p < .01$, with longer transit times (a sign of elasticity) associated with higher cerebral blood flow. This indicates that more elastic arteries lead to increased blood flow. Finally, average cerebral pulse transit time correlated with performance in the backward digit span, $r(28) = .397$, $p < .05$, and negatively with “failure-to-maintain set,” $r(28) = -.374$, $p < .05$, a scale of the WCST indicating the sudden disengagement of an appropriate task set, and therefore the failure to maintain working memory goals relevant to the task.

We examined specific relationships between the pulse transit time for particular brain arteries and neuropsychological variables. To increase statistical power, this particular analysis was based on the systole onset latency with respect to the EKG R wave (which was available in more participants than the carotid measurements). In this case, rather than

estimating all possible relationships (with a consequent large loss in statistical power or possibility of significantly inflating alpha error), we focused on two neuropsychological tests that can be linked to particular brain areas and networks, and on the arteries that are feeding such areas. Specifically, we selected the left middle cerebral artery—lMCA—and the superior portion of the precentral artery—sPCA, bilaterally. These two locations were selected because (a) they were easily visible in the pulsograms (see Figures 4B and 4C); and (b) they are close to areas of the brain that support functions investigated by some of the neuropsychological tests we used and which are known to be affected by aging: perisylvian brain regions in the left hemisphere support verbal processing (lMCA); dorsal prefrontal regions support attention control and working memory function (sPCA).

The pulse transit time in the lMCA was correlated with performance in the verbal fluency CFL task, $r(39) = .333$, $p < .05$ (this measure was not available in all participants because this region was on the border of the area covered by the optical probes in this study), and the pulse transit time in the sPCA was correlated with performance in the OSPAN task, $r(51) = .388$, $p < .005$, see Figure 7A and B). However, the pulse transit time of the lMCA was not correlated with performance in the OSPAN task, $r(39) = -.009$, *n.s.*) and that of sPCA was not correlated with performance in the CFL task, $r(51) = .036$, *n.s.*, supporting a double dissociation and indicating regional specificity. In other words, these results indicate that the pulse transit time in these arteries predicted functional changes only for tasks that were likely dependent on the cortical regions fed by these arteries. This in turn provides support for the idea that local variations in arterial elasticity may account for some of the variance in brain function in older adults.

Reliability of cerebral pulse estimates.—To estimate the reliability of the pulse parameters, we divided the recording periods into four segments, correlated them with each other (across participants), and applied the Spearman-Brown method to correct for a smaller test length, following the typical approach used for computing part-test reliability. The reliability of amplitude measures was $r(51) = .959$, $p < .0001$, which indicates that this parameter is highly stable. The reliability was weaker for the compliance estimates, $r(51) = .564$, $p < .0001$.

Figure 8A provides a comparison of pulsograms averaged separately for the odd and even participants. Although there are some local variations across the two groups, overall similar patterns are visible in them. To provide a statistical assessment of the reliability of the pulsograms, we determined whether there were points showing pulses consistently of larger or smaller magnitude than their neighboring points, when measured across participants. A statistical map showing the consistency of this “point versus neighbor” contrast across participants (in the form of z scores) is presented in Figure 8B. In this figure, any point with color indicates a $p < .05$ (this corresponds to an $r(52) > .267$). The points with the highest z scores had values of $z > 6.7$, corresponding to $r(52) > .75$. Note that these statistical maps are very similar to the thresholded average maps and to the maps for odd and even participants, supporting the consistency of these maps across participants.

Relationship between cerebral measures of arterial compliance/elasticity.—In this paper, we presented three measures of cerebral arterial function: pulse amplitude,

arterial compliance/elasticity, and pulse transit time. Globally, the amplitude measures did not correlate with the other measures: the correlations of cerebral pulse amplitude with compliance estimates was $t(51) = -.070$, and that with transit time was $t(28) = -.043$. The compliance estimates, however, correlated positively with pulse transit time, $t(28) = .378$, $p < .05$. This supports the idea that there are at least two separable components of arterial function in the brain: a factor generally related to pulse pressure and one related to arterial compliance/elasticity per se (see also Jennings, Tahmoush, & Redmond, 1980).

Discussion

The results presented in this paper provide support for the use of noninvasive optical imaging as a tool for studying the arterial pulse in the brain. By using spatial contrast enhancement and thresholding, we isolated the pulse as measured over relatively large arteries from the background activity (pulsogram). The optical pulse appears to be generated inside the skull, presumably by arteries running over the surface of the brain. Three pieces of evidence support this conclusion. First, the trajectory of the arteries as identified by the pulsograms corresponds to that of arteries running along the surface of the brain as identified using an MRI-based arteriogram. Second, the direction of blood flow along these arteries, as measured using peak latency estimates, also corresponds to the direction of flow in intracranial arteries. Third, the phase pulsograms (see supporting information) show a reduction in phase at the moment of the systolic pulse peak. As the systolic pulse peak is characterized by a maximum level of absorption, the data are consistent with a reduction of photons migrating along relatively long paths between the source and the detector. Such paths penetrate deeply into the head, and are likely to reach the brain. If the pulse measures were instead related to superficial phenomena, only short paths would be disrupted by the increase in absorption, resulting in an apparent increase in the phase delay of photons reaching the detector (see supporting information for more details on this set of results). Taken together, these data provide strong support for the use of noninvasive optical imaging methods to the study of the pulse in the cerebral cortex.

These findings are consistent with previous literature. Specifically, two previous studies provided support to the claim that the optical pulse recorded from the scalp surface is generated inside the skull. Themelis et al. (2007) carried out measures of change in optical pulse parameters during CO_2-enriched breathing in piglets in one hemisphere, while simultaneously using invasive measurements on the other hemisphere to observe changes occurring in the brain and surface. The optical imaging data were much better correlated with the deep than the superficial invasive measures (at least when source-detector distances greater than 1 cm were used). Ebihara et al. (2013) showed that noninvasive optical measures were sensitive to changes in cerebral blood flow occurring in patients with stroke. In summary, there is strong evidence that optical measures provide valid information about arterial phenomena occurring inside the skull.

Consistent with this evidence, the oxygenation data presented in the current study show that the pulse signal is related to a vascular compartment where blood is strongly saturated with oxygen (Figure 2D). This indicates that the optical measures of the pulse are related to arterial rather than capillary phenomena. In this sense, these measures differ from those

obtained with conventional fNIRS methods, which show a much smaller level of oxygen saturation (Safonova et al., 2004), and are therefore likely to be generated in the very small vessels diffused over the parenchyma.

Our data indicate that the amplitude of the optical pulse at the carotid, and to a lesser degree in the brain, is well correlated with pulse pressure across participants (i.e., with the difference between systolic and diastolic blood pressure measured at the forearm). Optical pulse amplitude (measured as the difference between the average diastolic maximum and systolic minimum) is also positively correlated with age. However, pulse amplitude is not strongly correlated with cerebral blood flow as measured with ASL MRI methods. This finding appears to contrast with the interpretation proposed by Themelis et al. (2007) that the derivative of pulse amplitude should be considered as a measure of blood flow. In fact, in our data the derivative of the pulse amplitude is highly correlated with its actual amplitude ($r > .9$), and both measures increase significantly with age, whereas ASL measurements typically show decreased cerebral blood flow in aging (e.g., Parkes, Rashid, Chard, & Tofts, 2004). To further clarify our interpretation, it is important to consider that blood flow is related to the volume of blood that is pushed forward over a certain period of time. Within each vascular compartment (large arteries, arterioles, capillaries, and veins), it is therefore influenced by both the speed of the blood movement and the total cross-section of the vascular compartment along which the blood is moving. In aging, the arteries become sclerotic, and peripheral resistance increases because of the reduced size of the arteriole and capillary beds. As a consequence, both blood speed (as predicted by the Moens-Korteweg equation) and pulse amplitude (as predicted by the Windkessel model) increase in the large arteries. According to the Windkessel model, the increase in pulse amplitude is not a reflection of increased blood flow, but rather it is due to the superimposition of the feed-forward impulse provided by the systolic push and the faster and overlapping reflected wave given by the increased peripheral resistance (see Izzo and Shikoff, 2001). The cross-section reduction in the arterioles and capillaries in aging results in an overall decrease in blood flow to the tissue, irrespective of changes in pulse velocity. As a consequence, across participants, increased speed of blood flow in the large arteries should be associated with reduced flow in the tissue. In our study, we observed a positive correlation across participants between pulse transit time in major cerebral arteries and blood flow as measured with ASL MRI methods. This means that participants with very fast transit times have indeed less tissue blood flow than participants with longer transit times. This is consistent with the use of pulse wave velocity as an indication of arterial stiffness (arteriosclerosis).

Cerebral arterial elasticity, as measured by the optical compliance estimates presented here, is well correlated with CRF. This finding was predicted, as the relationship between arterial and cardiorespiratory health is well established (Boreham et al., 2004; Gando et al., 2010; Quan et al., 2014). Our data also suggest that measures of cerebral arterial compliance/elasticity are good predictors of individual differences in both brain volume and performance in neuropsychological tests. Specifically, the compliance estimates were good predictors of general brain volume (both for gray and white matter, and for cortical and subcortical structures). This correlation was not significant when compliance was measured at the carotid. As this is a correlational (and not experimental) observation, it is not possible to determine whether the lack of arterial elasticity per se is the cause of the brain volumetric

reduction. As arterial elasticity is correlated with aging (negatively) and fitness (positively), other phenomena associated with aging and fitness may lead both to changes in arterial elasticity and cerebral volumes.

In this respect, more information can be obtained from the relationship between pulse transit time in specific arteries (such as the lMCA and the sPCA) and performance on the CFL verbal fluency and OSPAN tests, which are thought to depend, at least to some extent, on the brain areas fed by these arteries. The double-dissociation we observed regarding these relationships is difficult to account for by invoking generalized phenomena (such as an increase in cerebral trophic factors), and points instead to a specific role of arterial elasticity in mediating at least some of the effects of aging and fitness on cognition. Of course, the relatively small sample used in the current study prevents us from reaching more definite conclusions. However, these findings are suggestive of a mediating role of arterial elasticity in the cognitive decline observed in old age and on the role of cardiorespiratory fitness as a protective factor.

The results of this study show a clear dissociation between cerebral pulse amplitude measures (which are positively correlated with pulse pressure and age, do not correlate with CRF and blood flow, and are poor predictors of brain anatomy and function) and pulse measures of cerebral arterial compliance/elasticity (which are modestly correlated with age, but show clear correlations with ASL estimates of blood flow and CRF, and are good predictors of brain anatomy and, to some degree, function), and are also correlated to each other. This may reflect the fact that pulse amplitude measures, just as blood pressure, are greatly influenced not only by long-term variables (such as arteriosclerosis) but also by a host of other factors related to general health and to the current state of the arterial system (e.g., vasodilation, vasoconstriction, etc.). The compliance estimates and pulse transit time, on the other hand, appear to be more selective indices of arterial elasticity/stiffness. This dissociation may be due, at least in part, to the fact that some of the participants used antihypertensive drugs (see footnote 2). Individuals who are prescribed blood pressure medications may display high levels of arteriosclerosis together with normal blood pressure values, which may lead to a reduction in the overall correlation between blood pressure and other variables. However, the estimates of arterial elasticity presented in this paper (compliance and pulse transit time) may not be influenced by the blood pressure medications and therefore may be more directly linked to arterial health.

The data also suggest that brain anatomy and function are more closely correlated with elasticity measures taken within the brain than with the analogous measures taken at the carotid. This suggests that there is an added value in using brain measures to examine arterial brain health with respect to using only more general measures. The data relating the elasticity of specific arteries (such as the lMCA and the sPCA) to specific neuropsychological test performance suggest that there may be even more to be gained by fractionating the cerebral arterial elasticity measures into their regional contributions. The pulse transit time measures appear particularly valuable in this respect, whereas the value of obtaining regional measures of compliance (rather than just averaging across the whole head) still remains to be ascertained. Part of the differences between the various measures

of elasticity may, however, depend on their respective reliability and on other measurement issues. A more extended analysis of these issues is needed.

This is the first paper reporting an extensive investigation of the use of optical imaging to analyze arterial health within the brain in a normal aging population. As such, this study shows promise but also has a number of limitations. Some of the limitations are intrinsic to optical measures: low penetration, making it impossible to analyze arteries deep in the brain; and relatively low spatial resolution compared to standard methods used in the field, such as MR angiography, ultrasound technology, and X-ray. The limited spatial resolution could be enhanced in the future by a denser recording array and sophisticated 3D-reconstruction methods, although it is likely to never reach the level of some of these established technologies. Nevertheless, optical methods provide a temporal resolution that is difficult to reach with MR technology, and are less invasive than X-ray methods, many of which involve the use of contrast agents. Optical technology can complement ultrasound technology by significantly extending the number of arteries and locations that can be investigated. Concurrent recording of these optical pulse parameters with both MR and ultrasound methods is also feasible and may enable a combined approach to achieve a more comprehensive analysis of arterial function. Finally, the possibility of obtaining them concurrently with neuroimaging measures during cognitive tasks may enhance the capabilities of aging and behavioral medicine research.

Other limitations are related to specific methodologies used in the current study. For instance, recordings from the carotids could only be obtained in a subset of the participants, because of the presence of movement artifacts and poor contact with the neck. Methodological advancements, such as more flexible optodes and better procedures for correcting artifacts, are likely to significantly improve the recordings.

Among the measures used, some, including the pulse amplitude measures, possessed a very high signal-to-noise ratio, and could be recorded very reliably. Others, however, including the arterial compliance measures, showed more limited reliability. It is likely that more sophisticated algorithms for their quantification could greatly improve the reliability of the compliance measures. In addition, our estimates of arterial compliance confounded in part the rate of relaxation of the arterial wall after the systole with the actual measure of the reflected wave. More advanced methods incorporating the direct estimation of parameters of the Windkessel model (see Thiele & Durieux, 2011; L. Wang, Xu, Feng, Meng, & Wang, 2013) may be able to tease apart these different aspects of compliance and elasticity.

The practical utility of noninvasive optical imaging as a tool for studying the brain’s vasculature depends in part on cost and availability issues. There are currently a large number (several hundreds) of noninvasive optical imaging devices available on the market and in laboratories scattered around the world, most of them used for recording fNIRS data. Most of these devices could be easily adapted to study pulse parameters, as the pulse is an easily detectable signal, which can be recorded with equipment that allows for the measurement of light intensity only (i.e., continuous-wave systems). A requirement for measuring pulse parameters is a sufficiently high sampling rate (at least 10–20 Hz); further, a relatively large number of channels (at least in the hundreds) is needed to generate the

pulsograms. Currently, the cost of this equipment may be comparable to that of some large EEG systems. An important practical aspect is that pulse measures can be obtained while simultaneously recording other optical signals, such as those related to neuronal activity (EROS and FOS; Gratton & Fabiani, 2010) or those related to tissue hemodynamics (such as fNIRS). This makes optical imaging a particularly attractive research tool for studying the interface between vascular and neuronal phenomena in aging and other at-risk populations (e.g., Fabiani et al., 2014).

In summary, the results of this study indicate that noninvasive optical imaging can be used to provide measures of the brain's arterial system, complementing other techniques such as MRI and ultrasound Doppler. Diffusive optical methods are noninvasive and relatively portable. They can provide concurrently a variety of parameters, such as pulse pressure, arterial elasticity, and speed of flow within the arteries. These measures can also be combined with measures of tissue oxygenation obtained with fNIRS (based on estimation of the tissue concentration of oxy- and deoxyhemoglobin; Murkin & Arango, 2009), and recorded concurrently with EEG and fMRI. By using a mapping approach, it is possible to identify and measure the characteristics of specific arteries running over the surface of the brain. The major limitation of noninvasive optical methods is their limited penetration (just a few centimeters from the surface of the head). However, the very high signal-to-noise ratio provided by the pulse signal may extend the penetration compared to other applications of optical imaging. This can be of particular utility in certain populations (such as preterm infants) in which the health of the arterial system is of great significance and difficult to study with other means. In addition to research uses, it may be possible in the future to develop clinical applications for these methods, especially in combination with other established methodologies.

Supplementary Material

Refer to Web version on PubMed Central for supplementary material.

Acknowledgments

We wish to acknowledge the support of National Institute of Aging (NIA) grant 1RC1AG035927 to M. Fabiani and Benjamin Zimmerman's support on National Science Foundation (NSF) IGERT training grant 0903622.

References

Alexander GE, Ryan L, Bowers D, Foster TC, Bizon JL, Geldmacher DS, & Glisky EL (2012). Characterizing cognitive aging in humans with links to animal models. Frontiers in Aging Neuroscience, 4, 21. doi: 10.3389/fnagi.2012.00021 [PubMed: 22988439]

Alian AA, & Shelley KH (2014). Photoplethysmography: Analysis of the pulse oximeter waveform. In Ehrenfeld JM & Cannesson M (Eds.), Monitoring technologies in acute care environments (pp. 165–178). New York, NY: Springer. doi: 10.1007/978-1-4614-8557-5_19

Allen J (2007). Photoplethysmography and its application in clinical physiological measurement. Physiological Measurement, 28, R1–R39. doi: 10.1088/0967-3334/28/3/R01 [PubMed: 17322588]

Andrews-Hanna JR, Snyder AZ, Vincent JL, Lustig C, Head D, Raichle ME, & Buckner RL (2007). Disruption of large-scale brain systems in advanced aging. Neuron, 56, 924–935. doi: 10.1016/j.neuron.2007.10.038 [PubMed: 18054866]

Asgari S, Gonzalez N, Subudhi AW, Hamilton R, Vespa P, Bergsneider M, … Hu X (2012). Continuous detection of cerebral vasodilatation and vasoconstriction using intracranial pulse morphological template matching. PloS ONE, 7, e50795. doi: 10.1371/journal.pone.0050795 [PubMed: 23226385]

Asmar R, Benetos A, Topouchian J, Laurent P, Pannier B, Brisac AM, … Levy BI (1995). Assessment of arterial distensibility by automatic pulse wave velocity measurement. Validation and clinical application studies. Hypertension, 26, 485–490. doi: 10.1161/01.HYP.26.3.485 [PubMed: 7649586]

Baniqued PL, Low KA, Fabiani M, & Gratton G (2013). Frontoparietal traffic signals: A fast optical imaging study of preparatory dynamics in response mode switching. Journal of Cognitive Neuroscience, 25, 887–902. doi: 10.1162/jocn_a_00341 [PubMed: 23249344]

Barnes DE, Yaffe K, Satariano WA, & Tager IB (2003). A longitudinal study of cardiorespiratory fitness and cognitive function in healthy older adults. Journal of the American Geriatrics Society, 51, 459–465. doi: 10.1046/j.1532-5415.2003.51153.x [PubMed: 12657064]

Beck AT, Steer RA, & Brown GK (1996). Manual for the Beck Depression Inventory (2nd ed.). San Antonio, TX: The Psychological Corporation.

Bennett DA, Wilson RS, Schneider JA, Evans DA, Beckett LA, Aggarwal NT, … Bach J (2002). Natural history of mild cognitive impairment in older persons. Neurology, 59, 198–205. doi: 10.1212/WNL.59.2.198 [PubMed: 12136057]

Benton AL, & Hamsher K (1989). Multilingual aphasia examination manual Iowa City, IA: University of Iowa.

Bherer L, Erickson KI, & Liu-Ambrose T (2013). A review of the effects of physical activity and exercise on cognitive and brain functions in older adults. Journal of Aging Research, Article ID 657508, 1–8. doi: 10.1155/2013/657508

Blacher J, Asmar R, Djane S, London GM, & Safar ME (1999). Aortic pulse wave velocity as a marker of cardiovascular risk in hypertensive patients. Hypertension, 33, 1111–1117. doi: 10.1161/01.HYP.33.5.1111 [PubMed: 10334796]

Blacher J, Guerin AP, Pannier B, Marchais SJ, Safar ME, & London GM (1999). Impact of aortic stiffness on survival in end-stage renal disease. Circulation, 99, 2434–2439. doi: 10.1161/01.CIR.99.18.2434 [PubMed: 10318666]

Black JE, Isaacs KR, Anderson BJ, Alcantara AA, & Greenough WT (1990). Learning causes synaptogenesis, whereas motor activity causes angiogenesis, in cerebellar cortex of adult rats. Proceedings of the National Academy of Sciences of the United States of America, 87, 5568–5572. doi: 10.1073/pnas.87.14.5568 [PubMed: 1695380]

Boreham CA, Ferreira I, Twisk JW, Gallagher AM, Savage MJ, & Murray LJ (2004). Cardiorespiratory fitness, physical activity, and arterial stiffness: The Northern Ireland Young Hearts Project. Hypertension, 44, 721–726. doi: 10.1161/01.HYP.0000144293.40699.9a [PubMed: 15452034]

Cabeza R (2002). Hemispheric asymmetry reduction in older adults: The HAROLD model. Psychology and Aging, 17, 85–100. doi: 10.1037/0882-7974.17.1.85 [PubMed: 11931290]

Calabia J, Torguet P, Garcia M, Garcia I, Martin N, Guasch B, … Valles M (2011). Doppler ultrasound in the measurement of pulse wave velocity: Agreement with the Complior method. Cardiovascular Ultrasound, 9, 1–6. doi: 10.1186/1476-7120-9-13 [PubMed: 21244654]

Calamante F, Thomas DL, Pell GS, Wiersma J, & Turner R (1999). Measuring cerebral blood flow using magnetic resonance imaging techniques. Journal of Cerebral Blood Flow and Metabolism, 19, 701–735. doi: 10.1097/00004647-199907000-00001 [PubMed: 10413026]

Casserly I, & Topol E (2004). Convergence of atherosclerosis and Alzheimer's disease: Inflammation, cholesterol, and misfolded proteins. Lancet, 363, 1139–1146. doi: 10.1016/S0140-6736(04)15900-X [PubMed: 15064035]

Colcombe SJ, Erickson KI, Scalf PE, Kim JS, Prakash R, McAuley E, … Kramer AF (2006). Aerobic exercise training increases brain volume in aging humans. The Journals of Gerontology. Series A, Biological Sciences and Medical Sciences, 61, 1166–1170. doi: 10.1093/gerona/61.11.1166 [PubMed: 17167157]

Colcombe S, & Kramer AF (2003). Fitness effects on the cognitive function of older adults: A meta-analytic study. Psychological Science, 14, 125–130. doi: 10.1111/1467-9280.t01-1-01430 [PubMed: 12661673]

Cook LB (2001). Extracting arterial flow waveforms from pulse oximeter waveforms apparatus. Anaesthesia, 56, 551–555. doi: 10.1046/j.1365-2044.2001.01986.x [PubMed: 11412161]

Corrigan JD, & Hinkeldey NS (1987). Relationships between parts A and B of the trail making test. Journal of Clinical Psychology, 43, 402–409. doi: 10.1002/1097-4679(198707)43:47<402::AID-JCLP2270430411>3.0.CO;2-E [PubMed: 3611374]

Cotman CW, Berchtold NC, & Christie L-A (2007). Exercise builds brain health: Key roles of growth factor cascades and inflammation. Trends in Neurosciences, 30, 464–472. doi: 10.1016/j.tins.2007.06.011 [PubMed: 17765329]

Cox RW (1996). AFNI: Software for analysis and visualization of functional magnetic resonance neuroimages. Computers and Biomedical Research, 29, 162–173. doi: 10.1006/cbmr.1996.0014 [PubMed: 8812068]

Dale AM, Fischl B, & Sereno MI (1999). Cortical surface-based analysis. I. Segmentation and surface reconstruction. NeuroImage, 9, 179–194. doi: 10.1006/nimg.1998.0395 [PubMed: 9931268]

de la Torre JC (1999). Critical threshold cerebral hypoperfusion causes Alzheimer's disease? Acta Neuropathologica, 98, 1–8. doi: 10.1007/s004010051044 [PubMed: 10412794]

Ebihara A, Tanaka Y, Konno T, Kawasaki S, Fujiwara M, & Watanabe E (2013). Detection of cerebral ischemia using the power spectrum of the pulse wave measured by near-infrared spectroscopy. Journal of Biomedical Optics, 18, 1–8. doi: 10.1117/1.JBO.18.10.106001

Erickson KI, Prakash RS, Voss MW, Chaddock L, Hu L, Morris KS, … Kramer AF (2009). Aerobic fitness is associated with hippocampal volume in elderly humans. Hippocampus, 19, 1030–1039. doi: 10.1002/hipo.20547 [PubMed: 19123237]

Erickson KI, Voss MW, Prakash RS, Basak C, Szabo A, Chaddock L, … Kramer AF (2011). Exercise training increases size of hippocampus and improves memory. Proceedings of the National Academy of Sciences, 108, 3017–3022. doi: 10.1073/pnas.1015950108

Fabiani M (2012). It was the best of times, it was the worst of times: A psychophysiologist's view of cognitive aging. Psychophysiology, 49, 283–304. doi: 10.1111/j.1469-8986.2011.01331.x [PubMed: 22220910]

Fabiani M, Gordon BA, Maclin EL, Pearson MA, Brumback-Peltz CR, Low KA, … Gratton G (2014). Neurovascular coupling in normal aging: A combined optical, ERP and fMRI study. NeuroImage, 85, 592–607. doi: 10.1016/j.neuroimage.2013.04.113 [PubMed: 23664952]

Ferreira I, Boreham CA, & Stehouwer CDA (2006). The benefits of exercise for arterial stiffness. American Journal of Hypertension, 19, 1037–1038. doi: 10.1016/j.amjhyper.2006.04.014 [PubMed: 17027824]

Fischl B, & Dale AM (2000). Measuring the thickness of the human cerebral cortex from magnetic resonance images. Proceedings of the National Academy of Sciences, 97, 11050–11055. doi: 10.1073/pnas.200033797

Fischl B, Liu A, & Dale AM (2001). Automated manifold surgery: Constructing geometrically accurate and topologically correct models of the human cerebral cortex. IEEE Transactions on Medical Imaging, 20, 70–80. doi: 10.1109/42.906426 [PubMed: 11293693]

Fischl B, Salat DH, Busa E, Albert M, Dieterich M, Haselgrove C, … Dale AM (2002). Whole brain segmentation: Automated labeling of neuroanatomical structures in the human brain. Neuron, 33, 341–355. doi: 10.1016/S0896-6273(02)00569-X [PubMed: 11832223]

Fletcher MA, Low KA, Boyd R, Zimmerman B, Gordon BA, Tan CH, … Fabiani M (2014). The effects of fitness on the entire aging brain: A volumetric and cortical thinning study Manuscript in preparation.

Gando Y, Kawano H, Yamamoto K, Sanada K, Tanimoto M, Oh T, … Miyachi M (2010). Age and cardiorespiratory fitness are associated with arterial stiffening and left ventricular remodelling. Journal of Human Hypertension, 24, 197–206. doi: 10.1038/jhh.2009.57 [PubMed: 19609287]

Gauthier S, Reisberg B, Zaudig M, Petersen RC, Ritchie K, Broich K, … International Psychogeriatric Association Expert Conference on Mild Cognitive Impairment. (2006). Mild cognitive impairment. Lancet, 367, 1262–1270. doi: 10.1016/S0140-6736(06)68542-5 [PubMed: 16631882]

Gordon BA, Rykhlevskaia EI, Brumback CR, Lee Y, Elavsky S, Konopack JF, … Fabiani M (2008). Neuroanatomical correlates of aging, cardiopulmonary fitness level, and education. Psychophysiology, 45, 825–838. doi: 10.1111/j.1469-8986.2008.00676.x [PubMed: 18627534]

Gratton E, Fantini S, Franceschini MA, Gratton G, & Fabiani M (1997). Measurements of scattering and absorption changes in muscle and brain. Philosophical Transactions of the Royal Society B: Biological Sciences, 352, 727–735. doi: 10.1098/rstb.1997.0055

Gratton G, & Corballis PM (1995). Removing the heart from the brain: Compensation for the pulse artifact in the photon migration signal. Psychophysiology, 32, 292–299. doi: 10.1111/j.1469-8986.1995.tb02958.x [PubMed: 7784538]

Gratton G, & Fabiani M (2010). Fast optical imaging of human brain function. Frontiers in Human Neuroscience, 4, article 52. doi: 10.3389/fnhum.2010.00052

Greenough WT, & Volkmar FR (1973). Pattern of dendritic branching in occipital cortex of rats reared in complex environments. Experimental Neurology, 40, 491–504. doi: 10.1016/0014-4886(73)90090-3 [PubMed: 4730268]

Grundman M, Petersen RC, Ferris SH, Thomas RG, Aisen PS, Bennett DA, … Alzheimer's Disease Cooperative Study. (2004). Mild cognitive impairment can be distinguished from Alzheimer disease and normal aging for clinical trials. Archives of Neurology, 61, 59–66. doi: 10.1001/archneur.61.1.59 [PubMed: 14732621]

Han X, Jovicich J, Salat D, van der Kouwe A, Quinn B, Czanner S, … Fischl B (2006). Reliability of MRI-derived measurements of human cerebral cortical thickness: The effects of field strength, scanner upgrade and manufacturer. NeuroImage, 32, 180–194. doi: 10.1016/j.neuroimage.2006.02.051 [PubMed: 16651008]

Hänninen T, Hallikainen M, Tuomainen S, Vanhanen M, & Soininen H (2002). Prevalence of mild cognitive impairment: A population-based study in elderly subjects. Acta Neurologica Scandinavica, 106, 148–154. doi: 10.1034/j.1600-0404.2002.01225.x [PubMed: 12174174]

Hatanaka R, Obara T, Watabe D, Ishikawa T, Kondo T, Ishikura K, … Imai Y (2011). Association of arterial stiffness with silent cerebrovascular lesions: The Ohasama study. Cerebrovascular Diseases, 31, 329–337. doi: 10.1159/000322599 [PubMed: 21212664]

Hayes SM, Hayes JP, Cadden M, & Verfaellie M (2013). A review of cardiorespiratory fitness-related neuroplasticity in the aging brain. Frontiers in Aging Neuroscience, 5. doi: 10.3389/fnagi.2013.00031

Heaton RK (1981). Wisconsin card sorting test manual, Odessa, FL: Psychological Assessment Resources, Inc.

Hedden T, & Gabrieli JDE (2004). Insights into the ageing mind: A view from cognitive neuroscience. Nature Reviews. Neuroscience, 5, 87–96. doi: 10.1038/nrn1323 [PubMed: 14735112]

Hernandez-Garcia L, Jahanian H, & Rowe DB (2010). Quantitative analysis of arterial spin labeling fMRI data using a general linear model. Magnetic Resonance Imaging, 28, 919–927. doi: 10.1016/j.mri.2010.03.035 [PubMed: 20456889]

Heyn P, Abreu BC, & Ottenbacher KJ (2004). The effects of exercise training on elderly persons with cognitive impairment and dementia: A meta-analysis. Archives of Physical Medicine and Rehabilitation, 85, 1694–1704. doi: 10.1016/j.apmr.2004.03.019 [PubMed: 15468033]

Hillman CH, Belopolsky AV, Snook EM, Kramer AF, & McAuley E (2004). Physical activity and executive control: Implications for increased cognitive health during older adulthood. Research Quarterly for Exercise and Sport, 75, 176–185. doi: 10.1080/02701367.2004.10609149 [PubMed: 15209336]

Hopkins ME, Davis FC, VanTieghem MR, Whalen PJ, & Bucci DJ (2012). Differential effects of acute and regular physical exercise on cognition and affect. Neuroscience, 215, 59–68. doi: 10.1016/j.neuroscience.2012.04.056 [PubMed: 22554780]

Hoshi Y, & Tamura M (1993). Detection of dynamic changes in cerebral oxygenation coupled to neuronal function during mental work in man. Neuroscience Letters, 150, 5–8. doi: 10.1016/0304-3940(93)90094-2 [PubMed: 8469403]

Huppert TJ, Diamond SG, Franceschini MA, & Boas DA (2009). HomER: A review of time-series analysis methods for near-infrared spectroscopy of the brain. Applied Optics, 48, D280–D298. doi: 10.1364/AO.48.00D280 [PubMed: 19340120]

Isaacs KR, Anderson BJ, Alcantara AA, Black JE, & Greenough WT (1992). Exercise and the brain: Angiogenesis in the adult rat cerebellum after vigorous physical activity and motor skill learning. Journal of Cerebral Blood Flow and Metabolism, 12, 110–119. doi: 10.1038/jcbfm.1992.14 [PubMed: 1370068]

Izzo JL, & Shikoff BE (2001). Arterial stiffness: Clinical relevance, measurement, and treatment. Review of Cardiovascular Medicine, 2, 29–40.

Jenkinson M, & Smith S (2001). A global optimisation method for robust affine registration of brain images. Medical Image Analysis, 5, 143–156. doi: 10.1016/S1361-8415(01)00036-6 [PubMed: 11516708]

Jennings JR, & Heim AF (2012). From brain to behavior: Hypertension's modulation of cognition and affect. International Journal of Hypertension. Article ID 701385, 1–12. doi: 10.1155/2012/701385

Jennings JR, Tahmoush AJ, & Redmond DP (1980). Noninvasive measurement of peripheral vascular activity. In Martin I & Venables PH, (Eds.), Techniques in psychophysiology (pp. 69–137). Chichester, UK: Wiley & Sons.

Jessberger S, & Gage FH (2008). Stem-cell-associated structural and functional plasticity in the aging hippocampus. Psychology and Aging, 23, 684–691. doi: 10.1037/a0014188 [PubMed: 19140640]

Jurca R, Jackson AS, LaMonte MJ, Morrow JR Jr., Blair SN, Wareham NJ, … Laukkanen R (2005). Assessing cardiorespiratory fitness without performing exercise testing. American Journal of Preventive Medicine, 29, 185–193. doi: 10.1016/j.amepre.2005.06.004

Kalaria RN, Akinyemi R, & Ihara M (2012). Does vascular pathology contribute to Alzheimer changes? Journal of the Neurological Sciences, 322, 141–147. doi: 10.1016/j.jns.2012.07.032 [PubMed: 22884479]

Kaufman AS, & Kaufman NL (2004). Kaufman brief intelligence test (2nd ed.). San Antonio, TX: The Psychological Corporation.

Keage HA, Churches OF, Kohler M, Pomeroy D, Luppino R, Bartolo ML, & Dement SE (2012). Cerebrovascular function in aging and dementia: A systematic review of transcranial Doppler studies. Geriatric Cognitive Diseases, 2, 258–270. doi: 10.1159/000339234

Keller HM, Meier WE, Anliker M, & Kumpe DA (1976). Noninvasive measurement of velocity profiles and blood flow in the common carotid artery by pulsed Doppler ultrasound. Stroke, 7, 370–377 [PubMed: 960155]

Kuperberg GR, Broome M, McGuire P, David A, Eddy M, Goff DC, … Fischl B (2003). Regionally localized thinning of the cerebral cortex in schizophrenia. Archives of General Psychiatry, 60, 878–888. doi: 10.1001/archpsyc.60.9.878 [PubMed: 12963669]

Levey A, Lah J, Goldstein F, Steenland K, & Bliwise D (2006). Mild cognitive impairment: An opportunity to identify patients at high risk for progression to Alzheimer's disease. Clinical Therapeutics, 28, 991–1001. doi: 10.1016/j.clinthera.2006.07.006 [PubMed: 16990077]

Liang Y-L, Teede H, Kotsopoulos D, & Shiel L (1998). Non-invasive measurements of arterial structure and function: Repeatability, interrelationships and trial sample size. Clinical Science, 95, 669–679. doi: 10.1042/CS19980148 [PubMed: 9831691]

Liddell BJ, Paul RH, Arns M, Gordon N, Kukla M, Rowe D, … Williams LM (2007). Rates of decline distinguish Alzheimer's disease and mild cognitive impairment relative to normal aging: Integrating cognition and brain function. Journal of Integrative Neuroscience, 6, 141–174. [PubMed: 17472227]

Lopez OL, Jagust WJ, DeKosky ST, Becker JT, Fitzpatrick A, Dulberg C, … Kuller LH (2003). Prevalence and classification of mild cognitive impairment in the Cardiovascular Health Study Cognition Study: Part 1. Archives of Neurology, 60, 1385–1389. doi: 10.1001/archneur.60.10.1385 [PubMed: 14568808]

Mailey EL, White SM, Wójcicki TR, Szabo AN, Kramer AF, & McAuley E (2010). Construct validation of a non-exercise measure of cardiorespiratory fitness in older adults. BMC Public Health, 10, 1–8. doi: 10.1186/1471-2458-10-59 [PubMed: 20043862]

Mattace-Raso FU, van der Cammen TJ, Hofman A, van Popele NM, Bos ML, Schalekamp MA, … Witteman JCM (2006). Arterial stiffness and risk of coronary heart disease and stroke: The Rotterdam study. Circulation, 113, 657–663. doi: 10.1161/CIRCULATIONAHA.105.555235 [PubMed: 16461838]

Mayeux R, Stern Y, Rosen J, & Leventhal J (1981). Depression, intellectual impairment and Parkinson's disease. Neurology, 31, 645–650. [PubMed: 7195481]

McAuley E, Kramer AF, & Colcombe SJ (2004). Cardiovascular fitness and neurocognitive function in older adults: A brief review. Brain, Behavior, and Immunity, 18, 214–220. doi: 10.1016/j.bbi.2003.12.007 [PubMed: 15116743]

McAuley E, Szabo AN, Mailey EL, Erickson KI, Voss M, White SM, … Kramer AF (2011). Non-exercise estimated cardiorespiratory fitness: Associations with brain structure, cognition, and memory complaints in older adults. Mental Health and Physical Activity, 4, 5–11. doi: 10.1016/j.mhpa.2011.01.001 [PubMed: 21808657]

Murkin JM, & Arango M (2009). Near-infrared spectroscopy as an index of brain and tissue oxygenation [Supplement 1]. British Journal of Anaesthesia, 103, i3–i13. doi: 10.1093/bja/aep299 [PubMed: 20007987]

Oldfield RC (1971). The assessment and analysis of handedness: The Edinburgh inventory. Neuropsychologia, 9, 97–113. [PubMed: 5146491]

Olopade CO, Mensah E, Gupta R, Huo D, Picchietti DL, Gratton E, & Michalos A (2007). Noninvasive determination of brain tissue oxygenation during sleep in obstructive sleep apnea: A near-infrared spectroscopic approach. Sleep, 30, 1747–1755. [PubMed: 18246984]

Ouyang C, & Sutton BP (2011). Pseudo-continuous transfer insensitive labeling technique. Magnetic Resonance Medicine, 66, 768–776. doi: 10.1002/mrm.22815

Park DC, Lautenschlager G, Hedden T, Davidson NS, Smith AD, & Smith PK (2002). Models of visuospatial and verbal memory across the adult life span. Psychology and Aging, 17, 299–320. doi: 10.1037/0882-7974.17.2.299 [PubMed: 12061414]

Parkes LM, Rashid W, Chard DT, & Tofts PS (2004). Normal cerebral perfusion measurements using arterial spin labeling: Reproducibility, stability, and age and gender effects. Magnetic Resonance Medicine, 51, 736–743. doi: 10.1002/mrm.20023

Pfefferbaum A, Sullivan EV, Hedehus M, Lim KO, Adalsteinsson E, & Moseley M (2000). Age-related decline in brain white matter anisotropy measured with spatially corrected echo-planar diffusion tensor imaging. Magnetic Resonance in Medicine, 44, 259–268. doi: 10.1002/1522-2594(200008)44:2<259::AID-MRM13>3.0.CO;2-6 [PubMed: 10918325]

Prakash RS, Snook EM, Motl RW, & Kramer AF (2010). Aerobic fitness is associated with gray matter volume and white matter integrity in multiple sclerosis. Brain Research, 1341, 41–51. doi: 10.1016/j.brainres.2009.06.063 [PubMed: 19560443]

Quan HL, Blizzard CL, Sharman JE, Magnussen CG, Dwyer T, Raitakari O, … Venn AJ (2014). Resting heart rate and the association of physical fitness with carotid artery stiffness. American Journal of Hypertension, 27, 65–71. doi: 10.1093/ajh/hpt161 [PubMed: 24029163]

Raz N, Ghisletta P, Rodrigue KM, Kennedy KM, & Lindenberger U (2010). Trajectories of brain aging in middle-aged and older adults: Regional and individual differences. NeuroImage, 51, 501–511. doi: 10.1016/j.neuroimage.2010.03.020 [PubMed: 20298790]

Rosas HD, Liu AK, Hersch S, Glessner M, Ferrante RJ, Salat DH, … Fischl B (2002). Regional and progressive thinning of the cortical ribbon in Huntington's disease. Neurology, 58, 695–701. doi: 10.1212/WNL.58.5.695 [PubMed: 11889230]

Safonova LP, Michalos A, Wolf U, Wolf M, Hueber DM, Choi JH, … & Gratton E (2004). Age-correlated changes in cerebral hemodynamics assessed by near-infrared spectroscopy. Archives of Gerontology and Geriatrics, 39, 207–225. doi: 10.1016/j.archger.2004.03.007 [PubMed: 15381340]

Salthouse TA (2010). Selective review of cognitive aging. Journal of the International Neuropsychological Society, 16, 754–760. doi: 10.1017/S1355617710000706 [PubMed: 20673381]

Schaie KW (1989). The hazards of cognitive aging. Gerontologist, 29, 484–493. doi: 10.1093/geront/29.4.484 [PubMed: 2521108]

Shipley WC (1940). A self-administering scale for measuring intellectual impairment and deterioration. Journal of Psychology, 9, 371–377.

Stamatakis E, Hamer M, O'Donovan G, Batty GD, & Kivimaki M (2013). A non-exercise testing method for estimating cardiorespiratory fitness. European Heart Journal, 34, 750–758. doi: 10.1093/eurheartj/ehs097 [PubMed: 22555215]

Swain RA, Harris AB, Wiener EC, Dutka MV, Morris HD, Theien BE, … Greenough WT (2003). Prolonged exercise induces angiogenesis and increases cerebral blood volume in primary motor cortex of the rat. Neuroscience, 117, 1037–1046. doi: 10.1016/S0306-4522(02)00664-4 [PubMed: 12654355]

Talairach J, & Tournoux P (1988). Co-planar stereotaxic atlas of the human brain. 3-Dimensional proportional system: An approach to cerebral imaging New York, NY: Thieme Medical Publishers.

Tien AY, Spevack TV, Jones DW, Pearlson GD, Schlaepfer TE, & Strauss ME (1996). Computerized Wisconsin card sorting test: Comparison with manual administration. Journal of Medical Sciences, 12, 479–485.

Themelis G, D'Arceuil H, Diamond SG, Thaker S, Huppert TJ, Boas DA, & Franceschini MA (2007). Near-infrared spectroscopy measurement of the pulsatile component of cerebral blood flow and volume from arterial oscillations. Journal of Biomedical Optics, 12, 014033. doi: 10.1117/1.2710250 [PubMed: 17343508]

Thiele RH, & Durieux ME (2011). Arterial waveform analysis for the anesthesiologist: Past, present, and future concepts. Anesthesia and Analgesia, 113, 766–776. doi: 10.1213/ANE.0b013e31822773ec [PubMed: 21890890]

Tse C-Y, Low KA, Fabiani M, & Gratton G (2012). Rules rule! Brain activity dissociates the representations of stimulus contingencies with varying levels of complexity. Journal of Cognitive Neuroscience, 24, 1941–1959. doi: 10.1162/jocn_a_00229 [PubMed: 22452560]

Tyndall AV, Davenport MH, Wilson BJ, Burek GM, Arsenault-Lapierre G, Haley E, … Poulin MJ (2013). The brain-in-motion study: Effect of a 6-month aerobic exercise intervention on cerebrovascular regulation and cognitive function in older adults. BMC Geriatrics, 13, 1–10. doi: 10.1186/1471-2318-13-21 [PubMed: 23280140]

Unsworth N, Heitz RP, Schrock JC, & Engle RW (2005). An automated version of the operation span task. Behavior Research Methods, 37, 498–505. doi: 10.3758/BF03192720 [PubMed: 16405146]

Unverzagt FW, McClure LA, Wadley VG, Jenny NS, Go RC, Cushman M, … Howard G (2011). Vascular risk factors and cognitive impairment in a stroke-free cohort. Neurology, 77, 1729–1736. doi: 10.1212/WNL.0b013e318236ef23 [PubMed: 22067959]

Vaitkevicius PV, Fleg JL, Engel JH, O'Connor FC, Wright JG, Lakatta LE, … Lakatta EG (1993). Effects of age and aerobic capacity on arterial stiffness in healthy adults. Circulation, 88, 1456–1462. doi: 10.1161/01.CIR.88.4.1456 [PubMed: 8403292]

Villringer A, & Chance B (1997). Non-invasive optical spectroscopy and imaging of human brain function. Trends in Neurosciences, 20, 435–442. doi: 10.1016/S0166-2236(97)01132-6 [PubMed: 9347608]

Voss MW, Prakash RS, Erickson KI, Basak C, Chaddock L, Kim JS, … Kramer AF (2010). Plasticity of brain networks in a randomized intervention trial of exercise training in older adults. Frontiers in Aging Neuroscience, 2. doi: 10.3389/fnagi.2010.00032

Voss MW, Vivar C, Kramer AF, & van Praag H (2013). Bridging animal and human models of exercise-induced brain plasticity. Trends in Cognitive Sciences, 17, 525–544. doi: 10.1016/j.tics.2013.08.001 [PubMed: 24029446]

Voss MW, Heo S, Prakash RS, Erickson KI, Alves H, Chaddock L, … Kramer AF (2013). The influence of aerobic fitness on cerebral white matter integrity and cognitive function in older adults: Results of a one-year exercise intervention. Human Brain Mapping, 34, 2972–2985. doi: 10.1002/hbm.22119 [PubMed: 22674729]

Wang L, Xu L, Feng S, Meng MQ-H, & Wang K (2013). Multi-Gaussian fitting for pulse waveform using weighted least squares and multi-criteria decision making method. Computers in Biology and Medicine 43, 1661–1672. doi: 10.1016/j.compbiomed.2013.08.004 [PubMed: 24209911]

Wang Z, Das SR, Xie SX, Arnold SE, Detre JA, Wolk DA, & Alzheimer's Disease Neuroimaging Initiative. (2013). Arterial spin labeled MRI in prodromal Alzheimer's disease: A multi-site study. NeuroImage: Clinical, 2, 630–636. doi: 10.1016/j.nicl.2013.04.014 [PubMed: 24179814]

Whalen C, Maclin EL, Fabiani M, & Gratton G (2008). Validation of a method for coregistering scalp recording locations with 3D structural MR images. Human Brain Mapping, 29, 1288–1301. doi: 10.1002/hbm.20465 [PubMed: 17894391]

Willum-Hansen T, Staessen JA, Torp-Pedersen C, Rasmussen S, Thijs L, Ibsen H, & Jeppesen J (2006). Prognostic value of aortic pulse wave velocity as index of arterial stiffness in the general population. Circulation, 113, 664–670. doi: 10.1161/CIRCULATIONAHA.105.579342 [PubMed: 16461839]

Wisely NA, & Cook LB (2001). Arterial flow waveforms from pulse oximetry compared with measured Doppler flow waveforms. Anaesthesia, 56, 556–561. doi: 10.1046/j.1365-2044.2001.01987.x [PubMed: 11412162]

Wolf U, Wolf M, Toronov V, Michalos A, Paunescu LA, & Gratton E (2000). Detecting cerebral functional slow and fast signals by frequency-domain near-infrared spectroscopy using two different sensors. OSA Biomedical Topical Meeting, Technical Digest (pp. 427–429).

Zhang Y, Brady M, & Smith S (2001). Segmentation of brain MR images through a hidden Markov random field model and the expectation maximization algorithm. IEEE Transactions in Medical Imaging, 20, 45–57. doi: 10.1109/42.906424

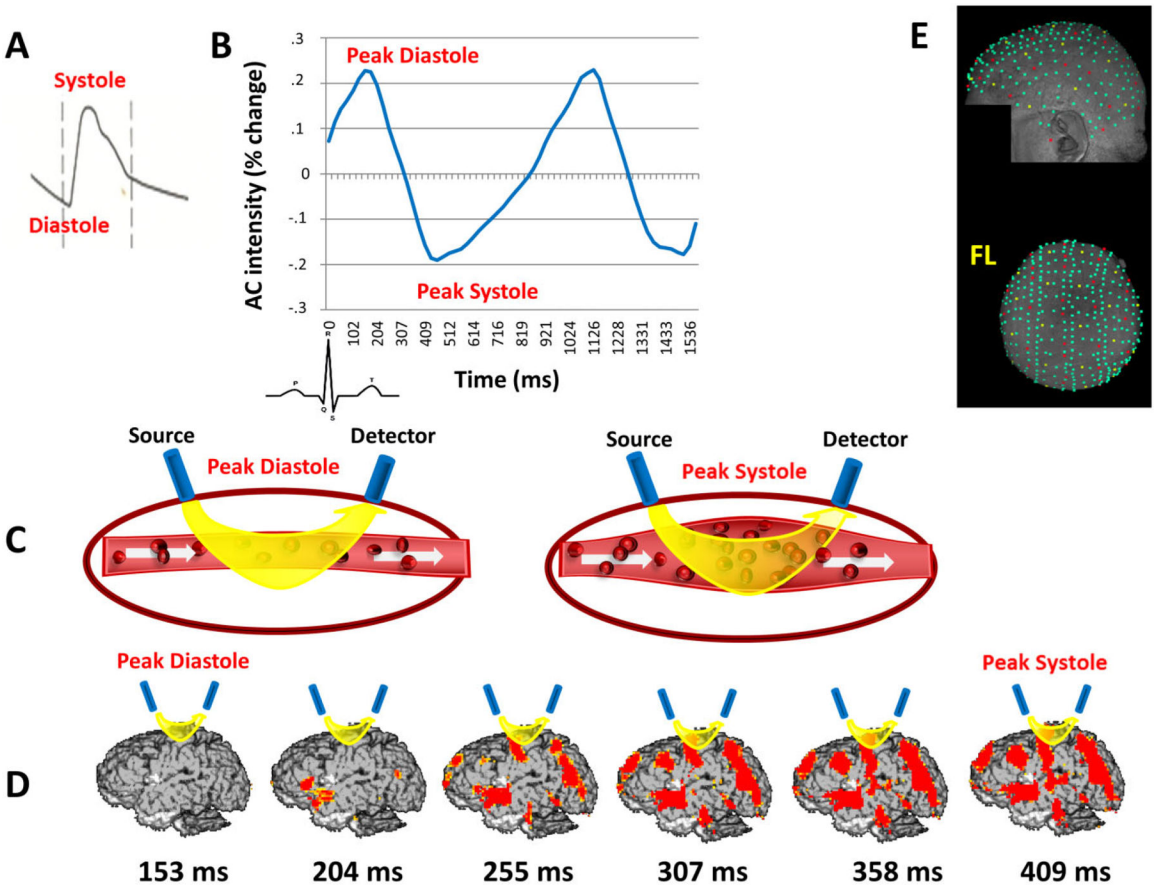

Figure 1.

A: Typical pulse wave as measured at the carotid by ultrasound Doppler. B: Pulse wave measured optically as a change in the intensity of the AC light moving between a source and a detector located on the surface of the head. The peak of the systole corresponds to a minimum (and the peak of the diastole to a maximum) in the amount of light detected after traveling through the tissue. C: Schematic depiction of changes in arterial diameter and oxyhemoglobin content during a pulse cycle, causing the changes in light intensity shown in (B), as more light is absorbed during the systole. D: Images of the pulse in the brain over time averaged across participants. Images are based on changes from the diastolic peak value (on average 153 ms after R wave onset). The systolic peak (on average 409 ms after R wave onset) shows the maximum change with respect to the diastolic peak value. At this point, the large arteries are most visible. E: Distribution of the sources (in yellow) and detectors (in red) used for data collection over the MR-rendered scalp of a representative participant. Other digitized locations used for coregistration with the structural MRI recordings are shown in green. FL = front left.

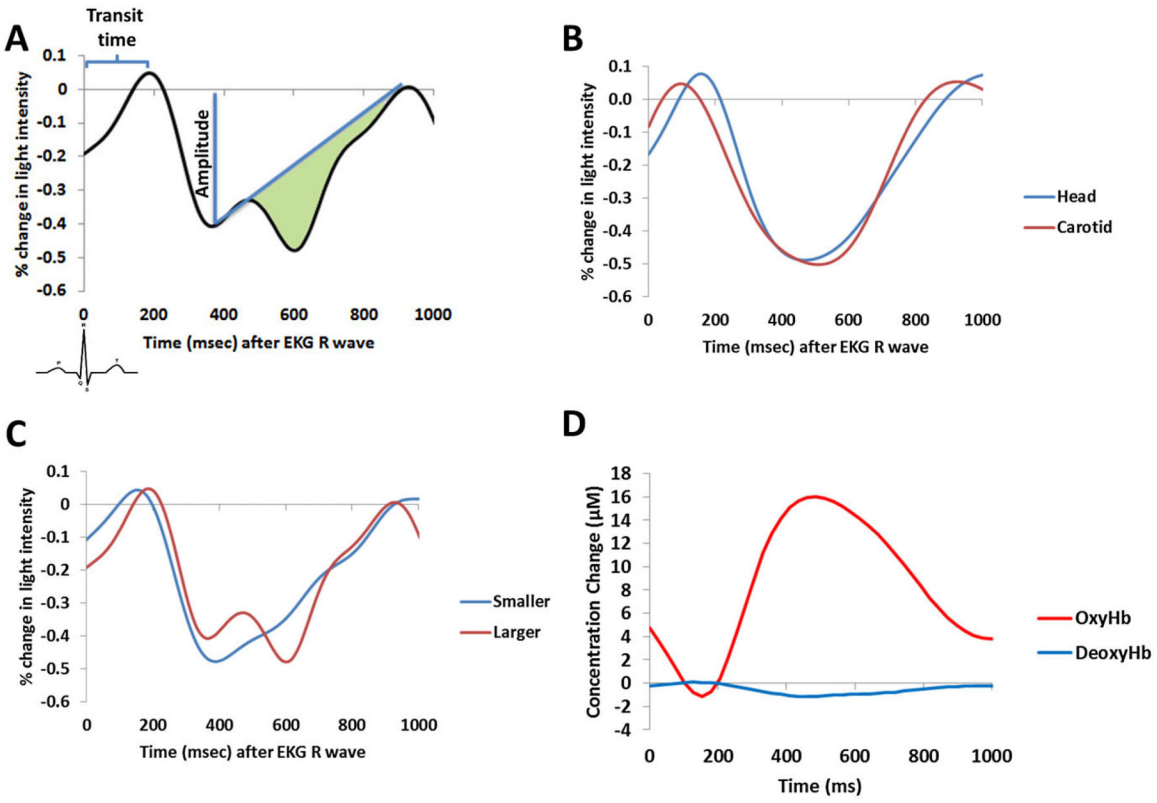

Figure 2.

A: Schematic depiction of the approaches used for pulse amplitude, transit time, and arterial compliance/elasticity measurements. The green area represents the estimated compliance/elasticity. B: Average pulse waveforms at the head and carotid. C: Cerebral pulse waveforms in two participants chosen for having a smaller or larger compliance. D: Average pulse waveform decomposed into its oxy- and deoxyhemoglobin contributions.

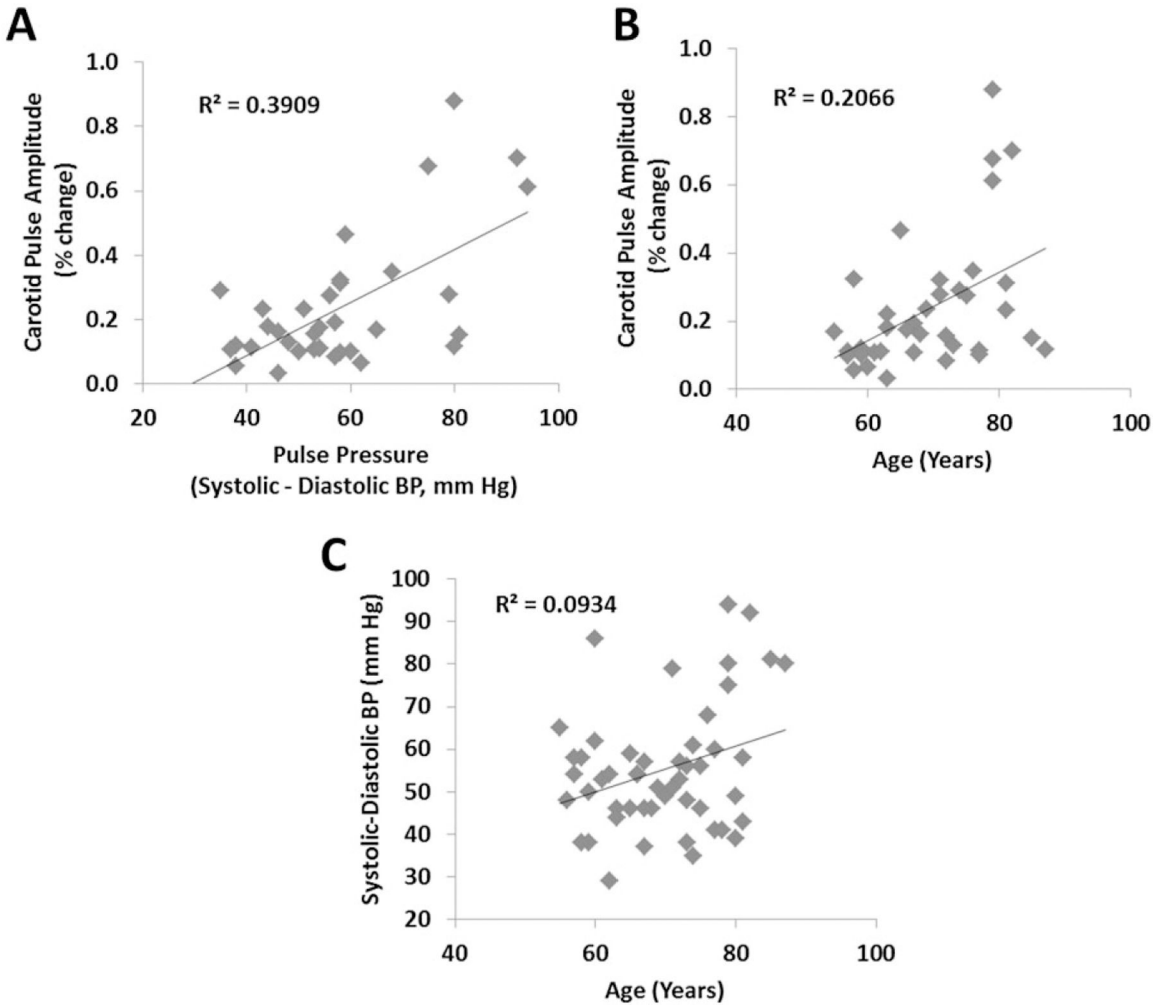

Figure 3.

Scatter plots depicting the relationships between carotid pulse amplitude and (A) systemic pulse pressure and (B) age. C: Scatter plot depicting the relationship between systemic pulse pressure and age.

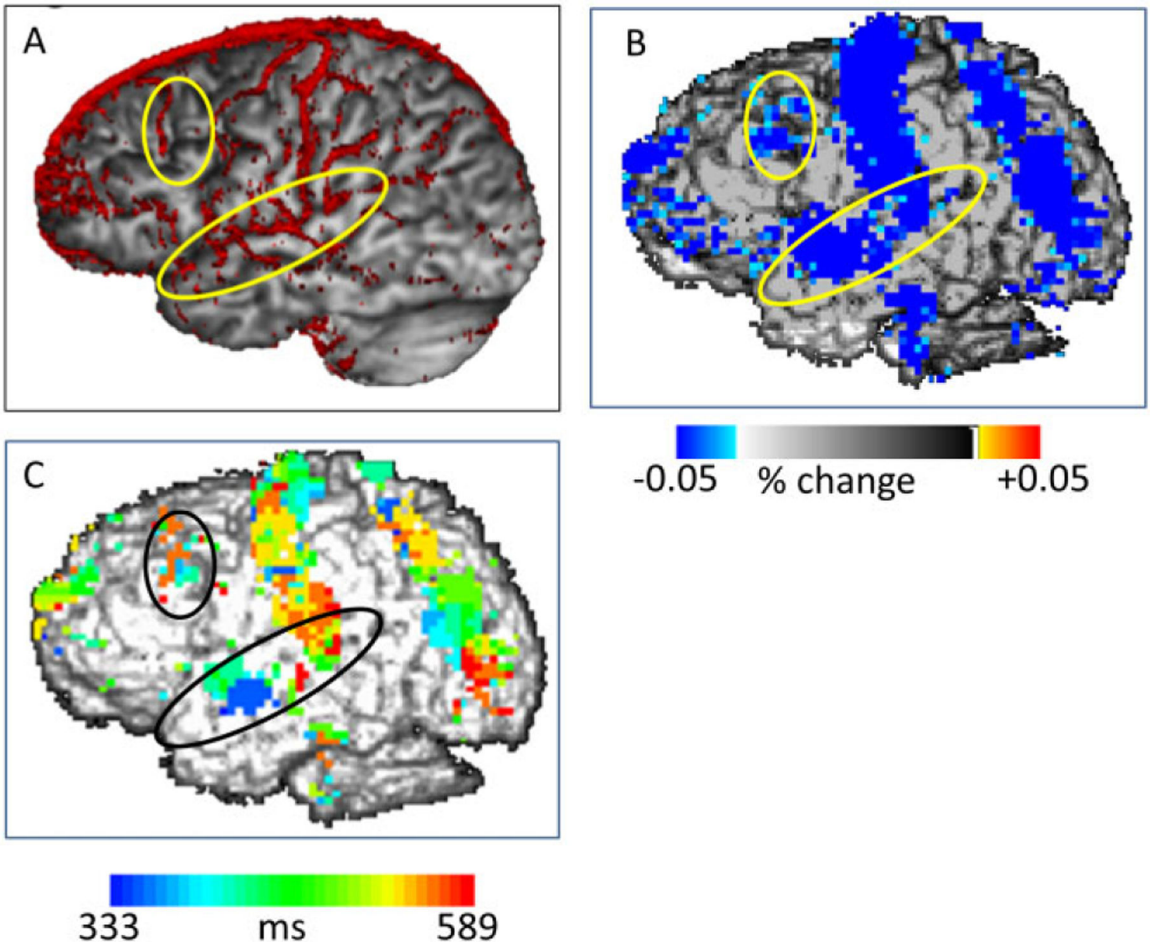

Figure 4.

A: MR arteriogram from one individual, in which deep and extracranial arteries have been masked. B: Optical pulsogram based on AC intensity values, averaged across participants. C: Time-resolved pulsogram, where colors indicate pulse transit times from the EKG R wave.

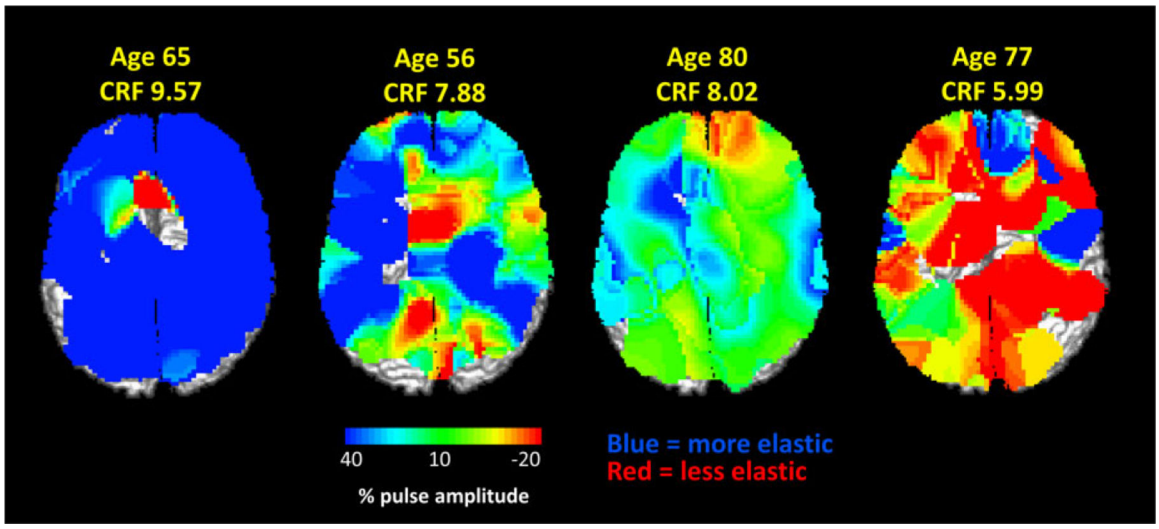

Figure 5.

Maps of the relative amplitude of the arterial compliance estimate, normalized by the peak of the systolic pulse, in four participants varying in age and CRF. Values in blue indicate greater compliance (corresponding to more elastic arteries), values in green and red indicate smaller compliance (corresponding to stiffer arteries). Higher CRF estimates indicate higher levels of fitness (adjusted for gender). Note the generally lower compliance in older and less fit individuals.

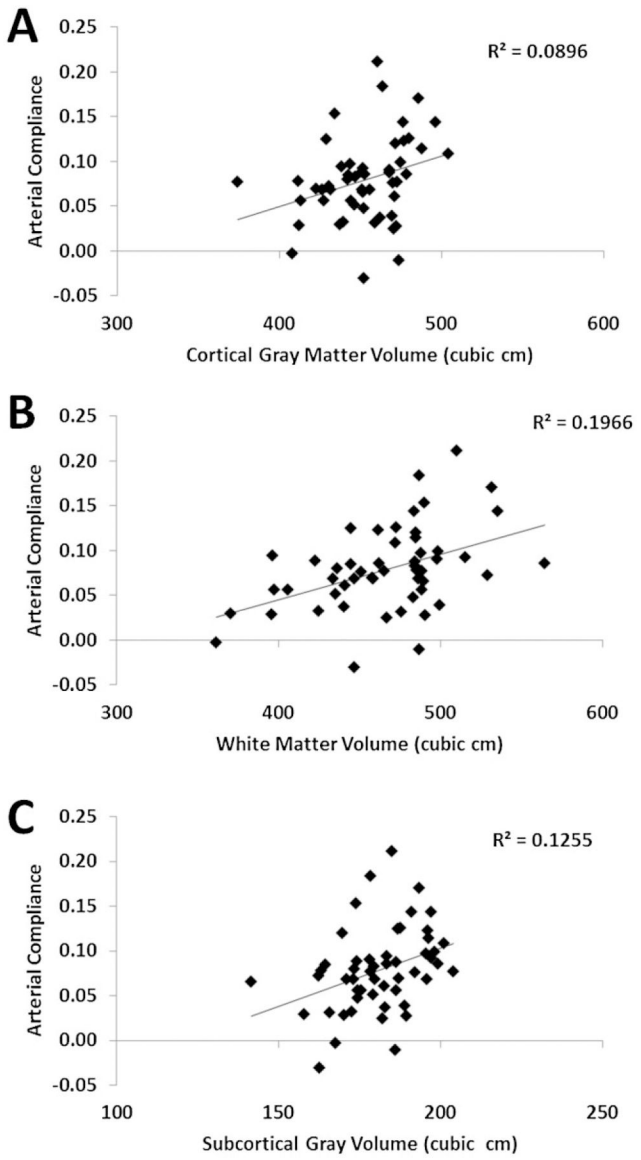

Figure 6.

Scatter plots depicting the correlations between arterial compliance and cortical gray matter volume (A), white matter volume (B), and subcortical gray volume (C). The positive correlations indicate that the larger the compliance (a sign of elasticity) the more preserved are the brain volumes.

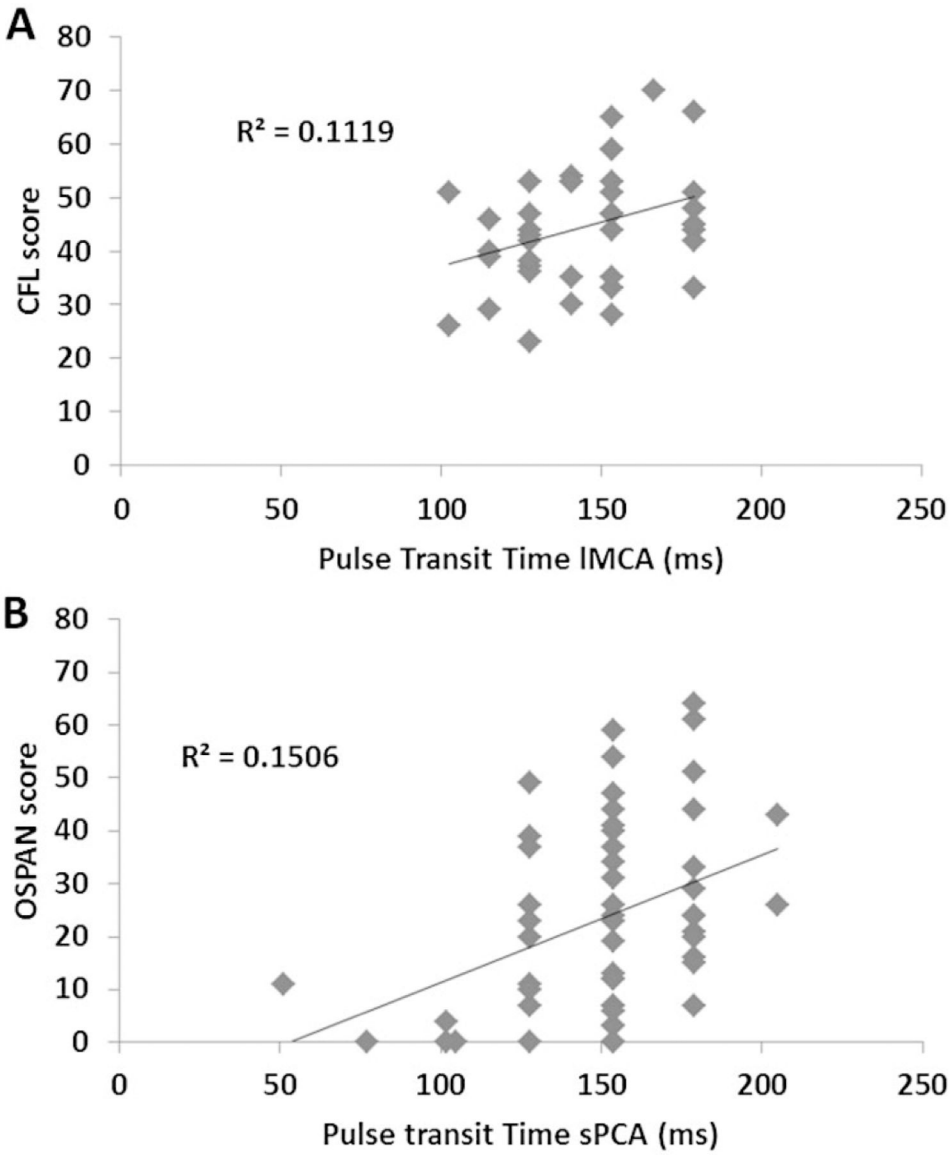

Figure 7.

Scatter plots showing the relationship between (A) pulse transit time in the left middle cerebral artery (lMCA) and verbal fluency performance, and (B) pulse transit time in the superior portion of the precentral artery (sPCA) and operation-span (OSPAN) performance. The positive correlations indicate that slower pulse transit times (a sign of elasticity) in specific arteries are associated with higher performance scores.

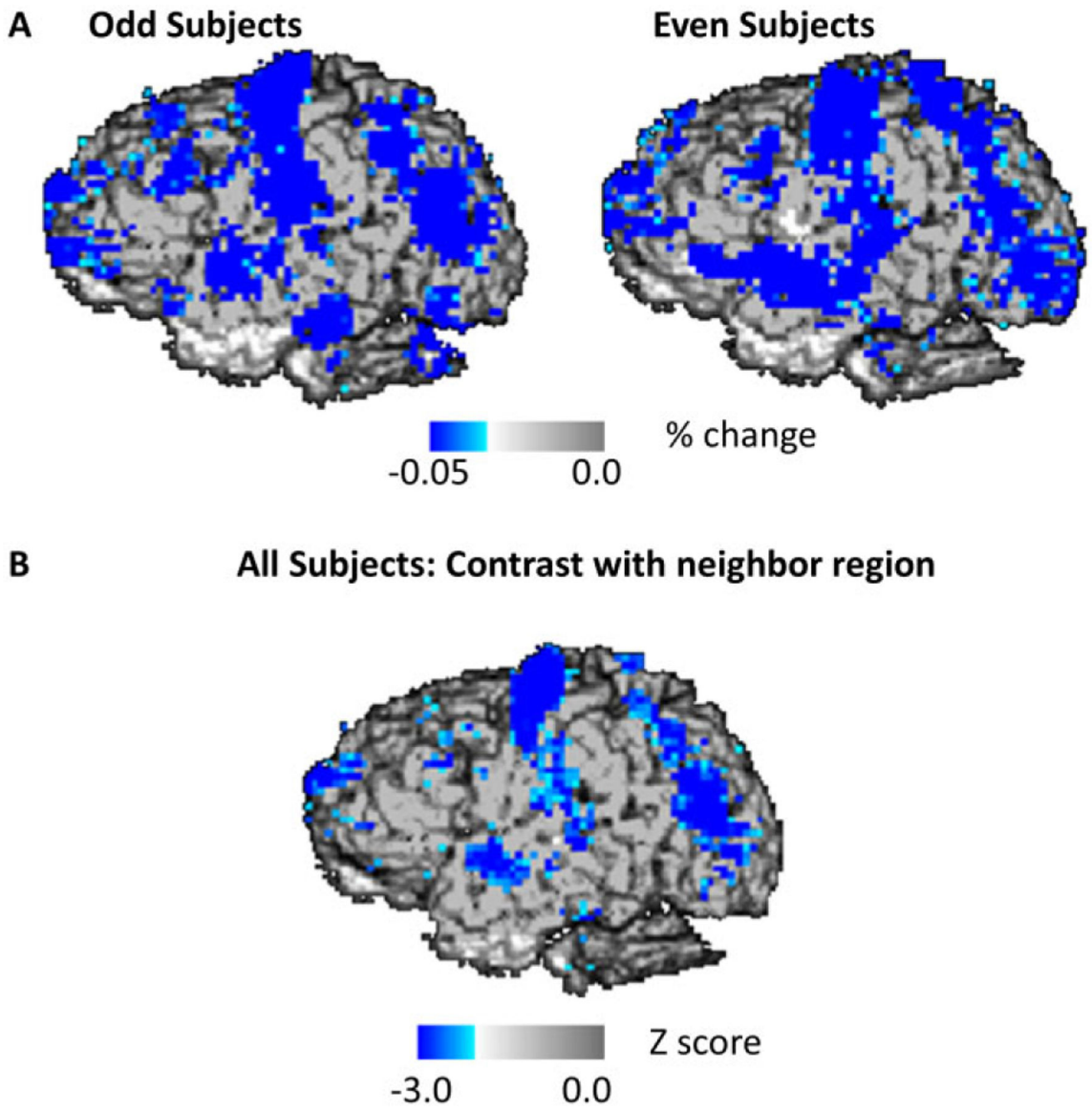

Figure 8.

A: Average optical pulsogram based on AC intensity values, averaged across odd and even participants. B: *Z*-score map obtained across participants, representing the difference between a voxel and the surrounding region. Values in blue indicate those voxels in which the amplitude of the pulse is consistently larger compared to the nearby voxels.

Table 1.

Demographic and Neuropsychological Characteristics

	Mean	*SD*	Range
Age (years)	69.53	8.34	55–87
Education (years)	16.82	2.83	12–20
CRF (metabolic equivalents, METs)	6.70	2.44	1.58–11.31
Body mass index	26.96	4.82	18.88–36.78
Physical activity score	1.00	1.08	0.00–3.03
Weight (in kg)	78.15	16.16	49.90–115.67
Height (in m)	1.70	.10	1.50–1.88
Systolic blood pressure	132.16	18.00	106–182
Diastolic blood pressure	76.90	9.84	61–95
Pulse pressure	55.26	14.99	29–94
Heart rate	72.05	10.95	53–95
Modified Mini-Mental Status exam (mMMS)	55.28	1.36	51–57
Beck’s Depression Index (BDI)	2.79	3.37	0–14
Shipley’s Vocabulary Test	35.98	2.53	30–40
Kaufman Brief Intelligent Test (K-BIT)	116.77	11.71	82–142
Verbal knowledge	56.00	2.88	45–60
Riddles	42.15	4.45	23–48
Matrices	36.08	4.76	23–45
Forward digit span	7.06	1.31	4–9
Backward digit span	5.30	1.20	3–8
Operation span (O-span)	24.17	17.88	0–64
Verbal fluency (CFL)	43.58	10.82	23–70
Trail Test A	18.23	5.70	9–35
Trail Test B	29.21	8.65	15–58
Trail B-A	10.98	6.87	−1–32
WCST (errors)	26.25	20.29	7–85

Note. $N = 53$ (27 females). Education capped at 20 years (postgraduate degree). The K-BIT score was normalized by age group (but not the subscores). *SD* = standard deviation; CRF = cardiorespiratory fitness; WCST = Wisconsin Card Sorting Test.

Table 2.

Summary of Significant Correlations Between the Optical Parameters of Arterial Pulse and Variables of Interest

	Carotids: Amplitude	Carotids: Transit time	Carotids: Compliance	Brain: Amplitude	Brain: Compliance
Carotids: Amplitude	–		−.319	.512	
Carotids: Transit time		–	.513		.348
Carotids: Compliance	−.319	.513	–		
Pulse Pressure (arm)	.625			.380	
CBF: Gray matter		.345			
CBF: White matter		.467			
Volume: Gray matter					.299
Volume: White matter					.443
Volume: Subcortical gray					.354
Age	.455			.382	−.390
Cardiorespiratory fitness (CRF)		.387			.416
Forward digit span			.368		
Backward digit span		.397			
WCST		−.374			

Table 3.

Correlations of Age and Cardiorespiratory Fitness (CRF) with Performance

Neuropsychological test	Age	CRF
mMMS	−0.181	0.107
Forward digit span	−0.262 +	0.165
Backward digit span	−0.256 +	0.339 *
OSPAN	−0.356 **	0.249 +
Trail A	0.396 **	−0.163
Trail B	0.505 **	−0.179
Trail B-Trail A	0.307 *	−0.090
CFL—Verbal fluency	−0.267 +	0.316 *
WCST		
Categories completed	−0.398 **	0.311 *
# Trials	0.477 **	−0.245 +
# Correct responses	0.125	−0.032
# Errors	0.437 **	−0.236 +
Perseverative responses	0.309 *	−0.138
Perseverative errors	0.342 +	−0.160
Nonperseverative errors	0.473 **	−0.276 *
% Perseverative errors	0.250 +	−0.131
Trials to complete 1st category	0.278 *	−0.348 *
% Conceptual errors	−0.395 **	0.223
Failure to maintain set	0.097	−0.221

+ $p < .10$

* $p < .05$

** $p < .01$.